

The atmospheric structure and fundamental parameters of Red Supergiants

B. Arroyo-Torres, M. Wittkowski,
J.M. Marcaide, and P. H. Hauschildt

University of Valencia
ESO
University of Hamburg

Introduction

Aims:

- Investigating the circumstellar environment of RSGs close to the photosphere and obtaining fundamental parameters and locating the stars in the HR diagram.

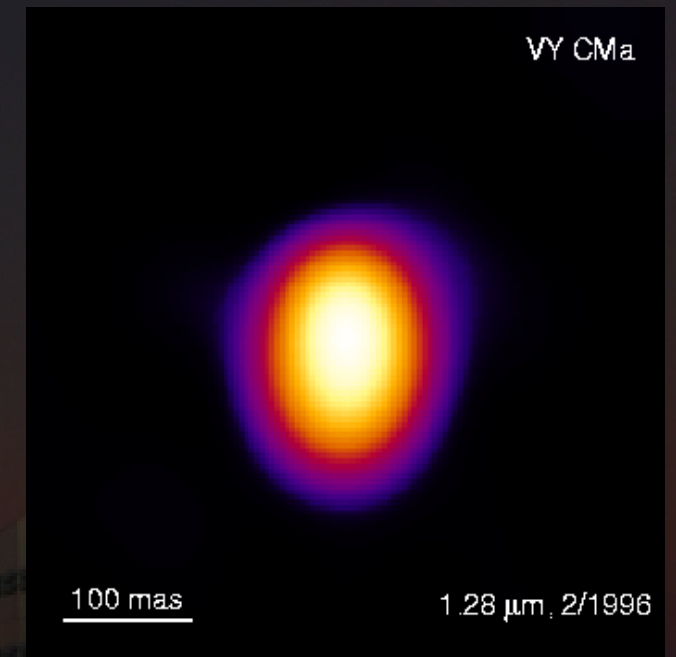
Previews works:

- *Levesque et al. 2005 & Massey et al. 2006*: spectrophotometric observations compared to MARCS models that caused a dramatic revision of the location of RSGs in the HR diagram.
- *Ohnaka et al. 2009, 2011*: presence of extended CO layers which can not be accounted for classical hydrostatic model atmospheres. (study of Betelgeuse)
- *Perrin et al. 2004, 2007 & Wittkowski et al. 2012*: extended and asymmetric water vapor layers.

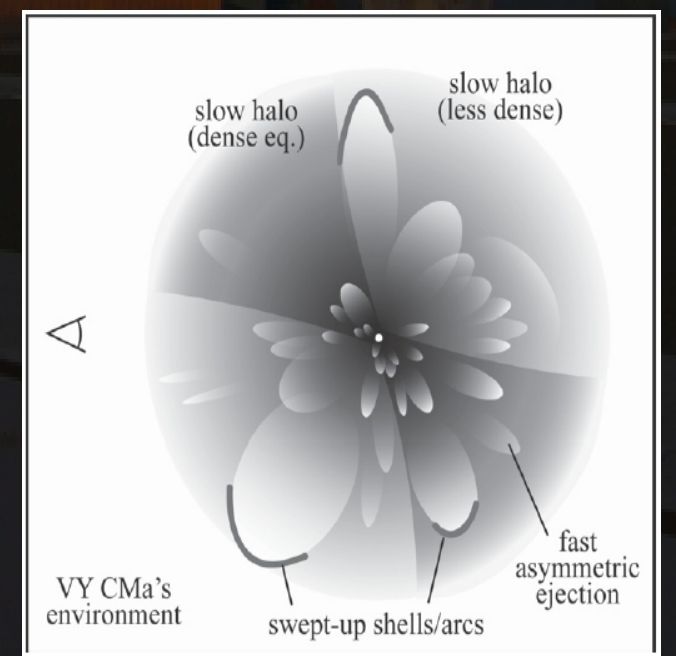
VY Canis Majoris

(Wittkowski et al. 2012, A&A, 540, L12)

- One of the most luminous and closest red supergiants in our Galaxy.
- Fundamental parameters have been discussed during the last decade with values between T_{eff} 2700 K and 3650 K, radii $600 R_{\text{sun}}$ and $3000 R_{\text{sun}}$, initial masses between $12 M_{\text{sun}}$ and $40 M_{\text{sun}}$
- Recent observations with new facilities like Herschel, SMA, APEX
- Exhibits a complex molecular environment
- Smith et al. (2009) propose a scenario of fast and dense CO/dust ejecta into a larger slow and less dense asymmetric envelope

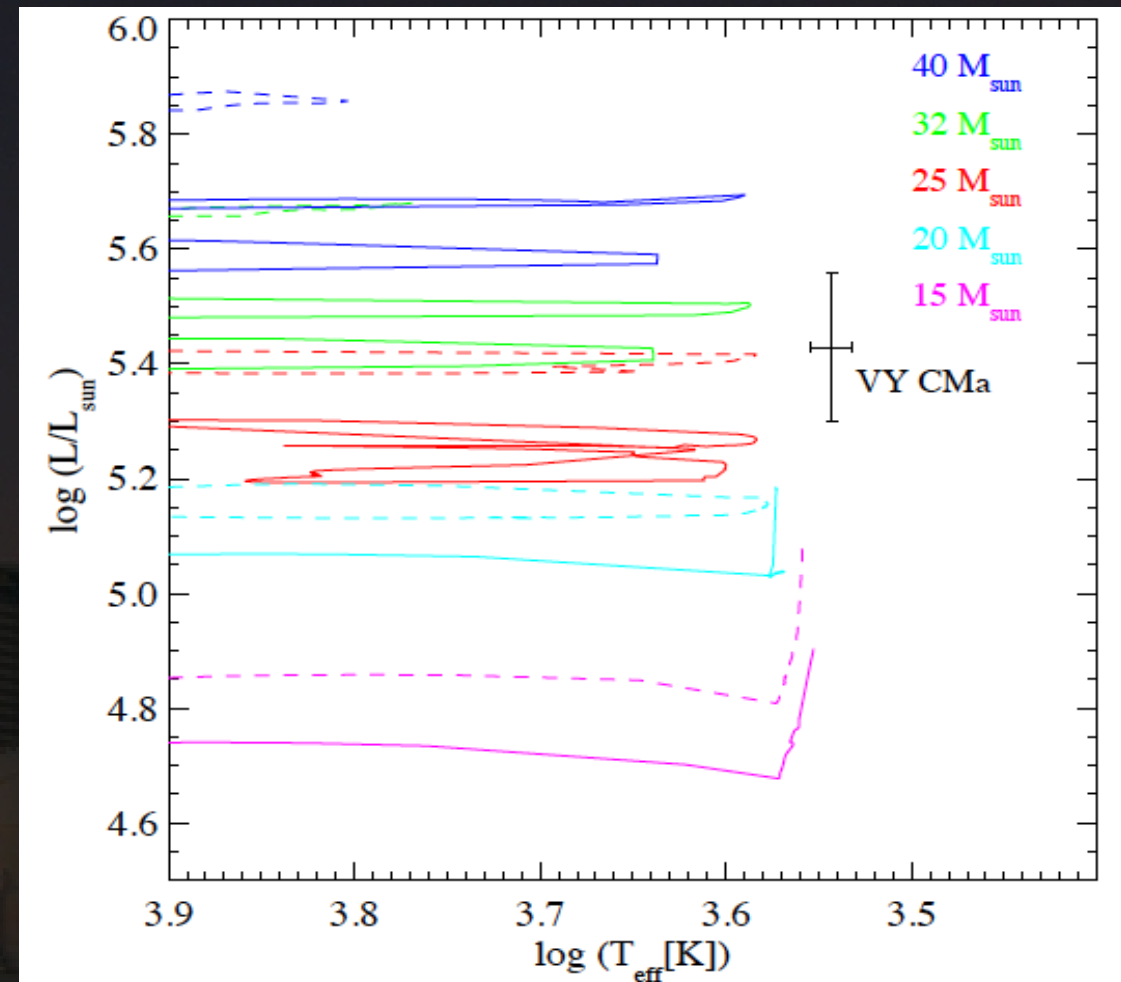
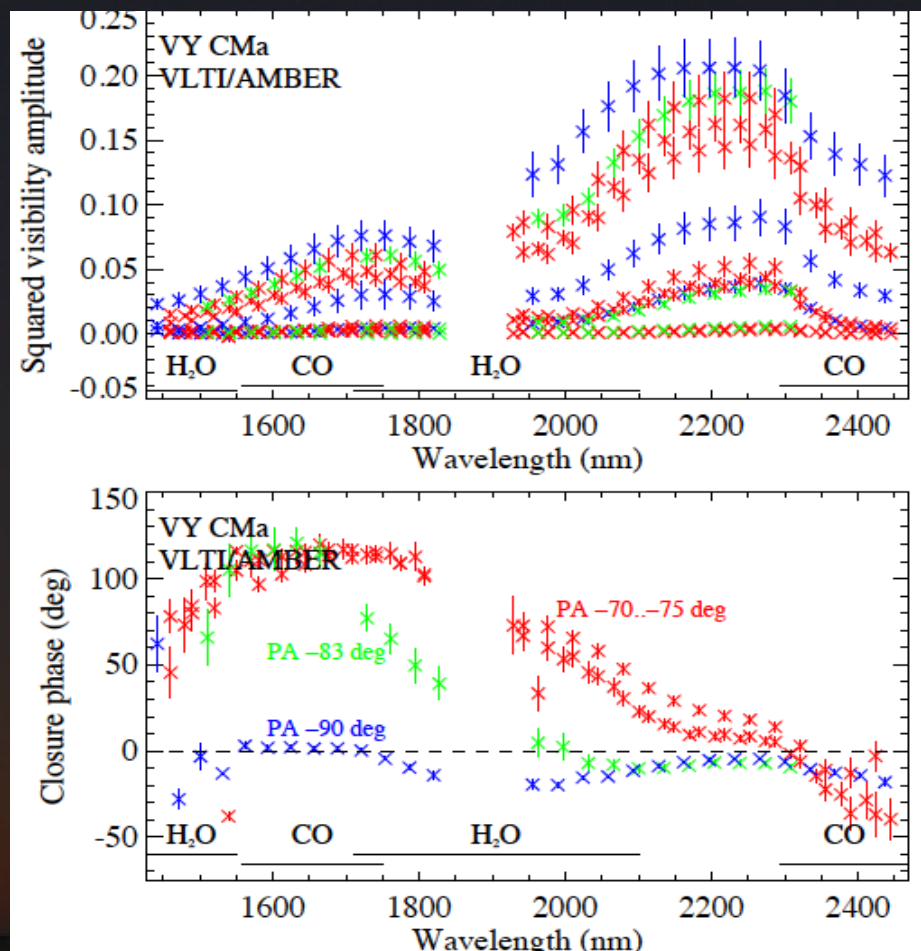


Wittkowski et al. 2008



Smith et al. 2009

VY Canis Majoris - Results



- Bumpy visibility curves, resembling those of AGB stars, indicative of atmospheric molecular layers (CO and H₂O)
- Closure phases indicative of deviations from point symmetry of atmospheric molecular layers.
- Revised fundamental parameters by isolating a near-continuum bandpass:

$$\Theta_{\text{Ross}} = 11.3 \pm 0.3 \text{ mas}, R_{\text{Ross}} = 1420 \pm 120 R_*, T_{\text{eff}} = 3490 \pm 90 \text{ K}$$

Our observations

	<i>calibrators</i>	<i>V</i> (mag)	<i>K</i> (mag)	<i>d</i> (pc)	<i>Sp.</i> <i>type</i>
AH Sco	tau Sgr	7,46	0,41	2260 (1)	M4
KW Sgr	HR 6583 / 11 Sgr	8,98	1,27	2400 (2)	M1.5 Ia
UY Sct	tau Sgr	9,00	0,73	2900 (3)	M4 Ia

* Medium resolution ($R \sim 1500$) in K-2.1 and K-2.3 μm with external fringe tracker FINITO

* We reduce our data with Amdlib and IDL scripts.

* We have also reduced the archival Betelgeuse data from 086.D-0351 (PI: Perrin - Jan 2011).

(1) Chen, X., Shen, Z.-Q., 2008, IAUS, 252, 247

(2) Melnik, A. M., Dambis, A. K., 2009, MNRAS, 400, 518

(3) Sylvester, C. J. et al. , 1998, MNRAS, 301, 1083

The PHOENIX Model

We use the version 16.03 of the PHOENIX code (Peter Hauschildt)

This model uses...

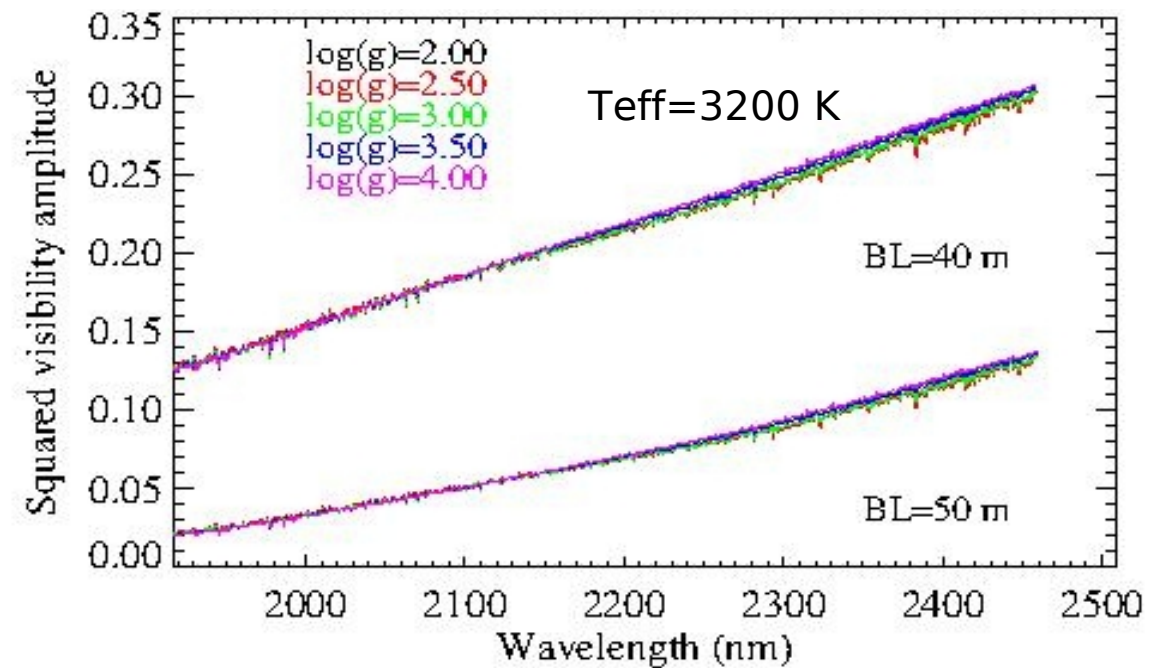
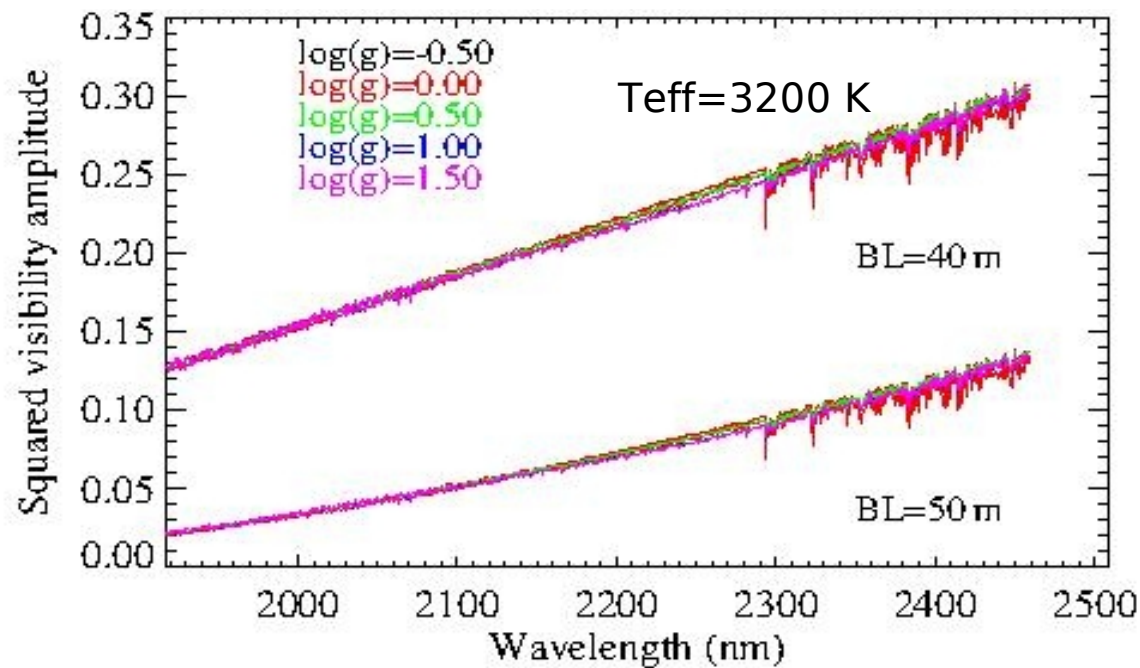
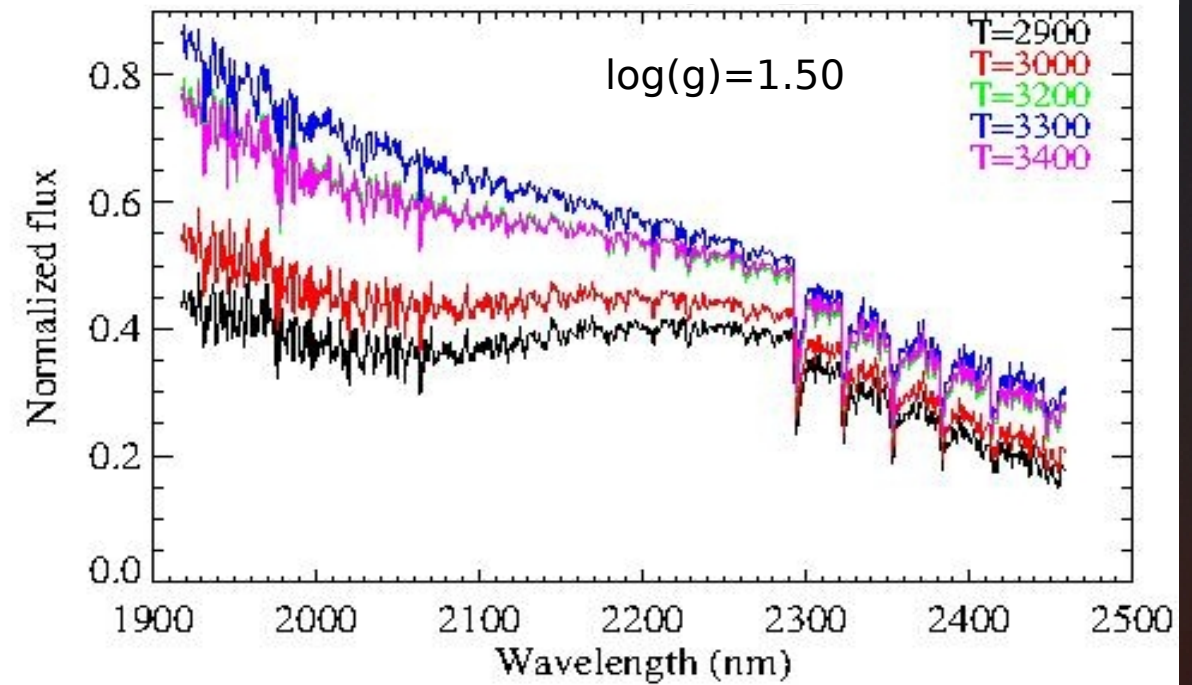
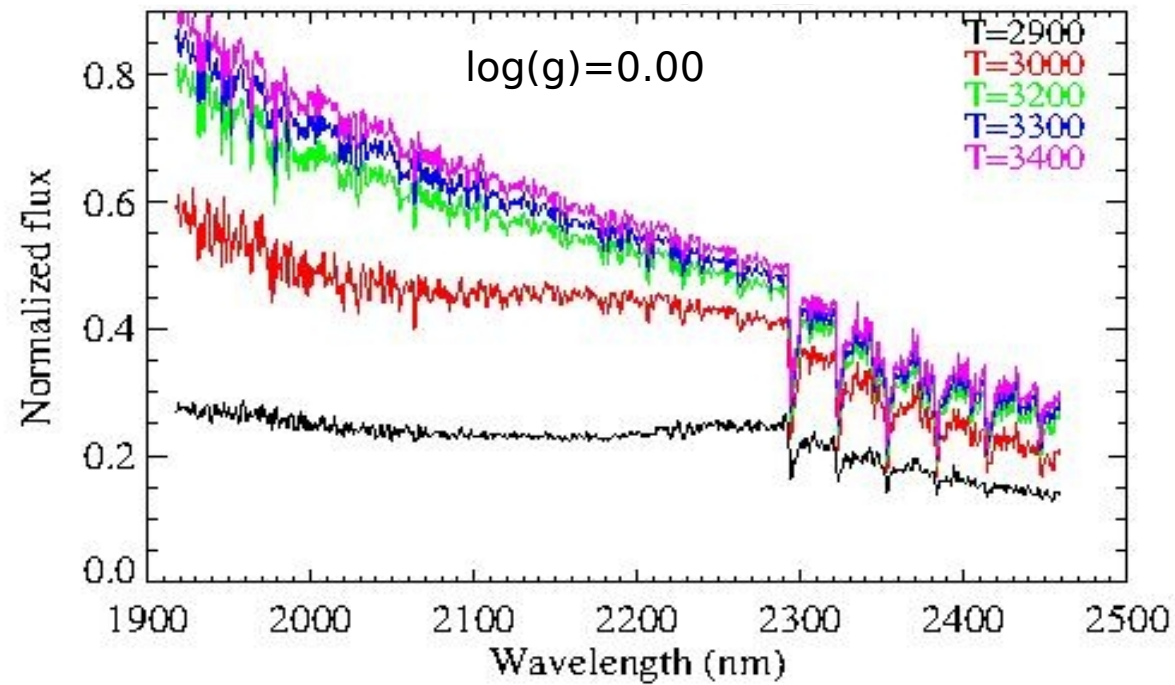
- Hydrostatic atmosphere
- Local thermodynamic equilibrium
- Spherical symmetry
- Limb-darkening effect

The model tabulates the intensity profile at 64 angles for wavelengths from 1.8 to 2.5 μm in steps of 0.01 \AA .

For working with the model, we must.....

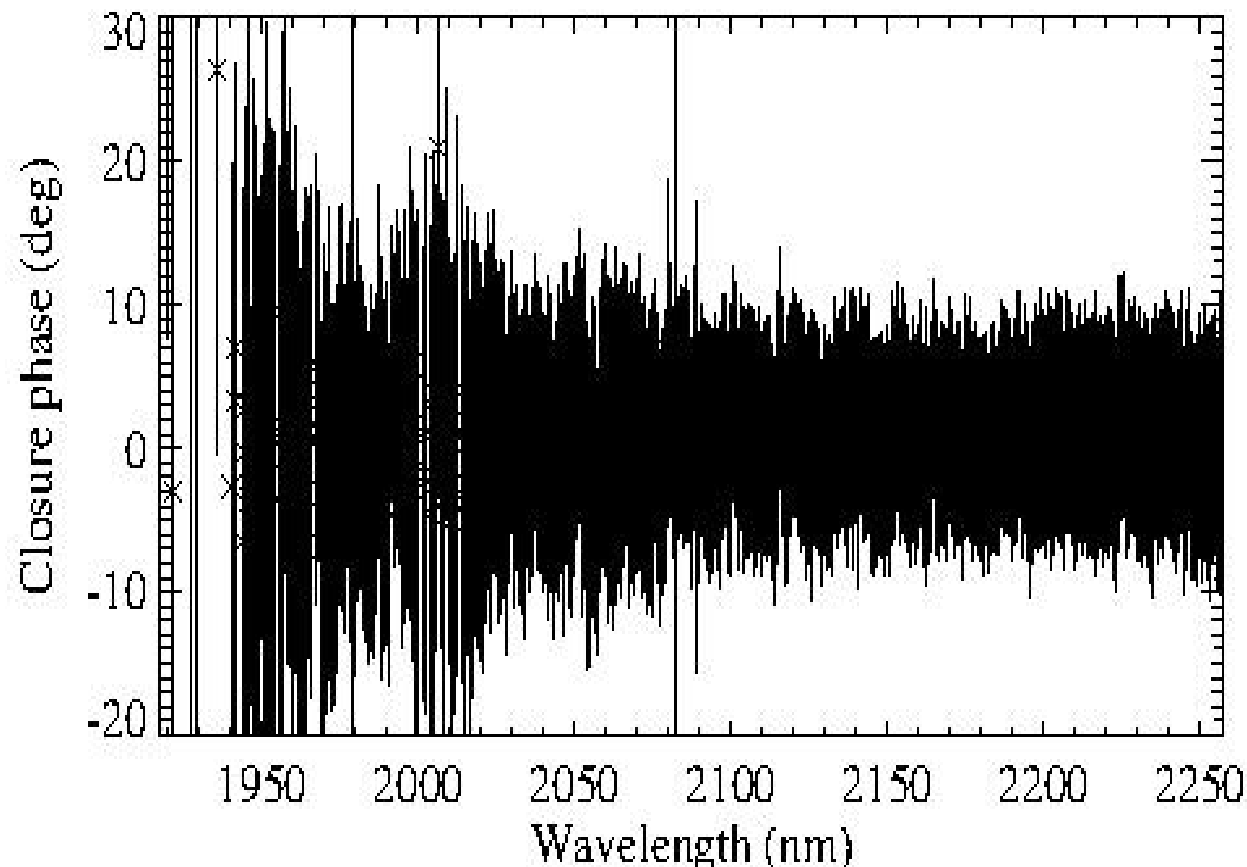
Average the monochromatic intensity profiles to match the spectral channel of the individual observations and compute the flux integrated over the stellar disk as the visibility values for the baseline used.

The PHOENIX Model

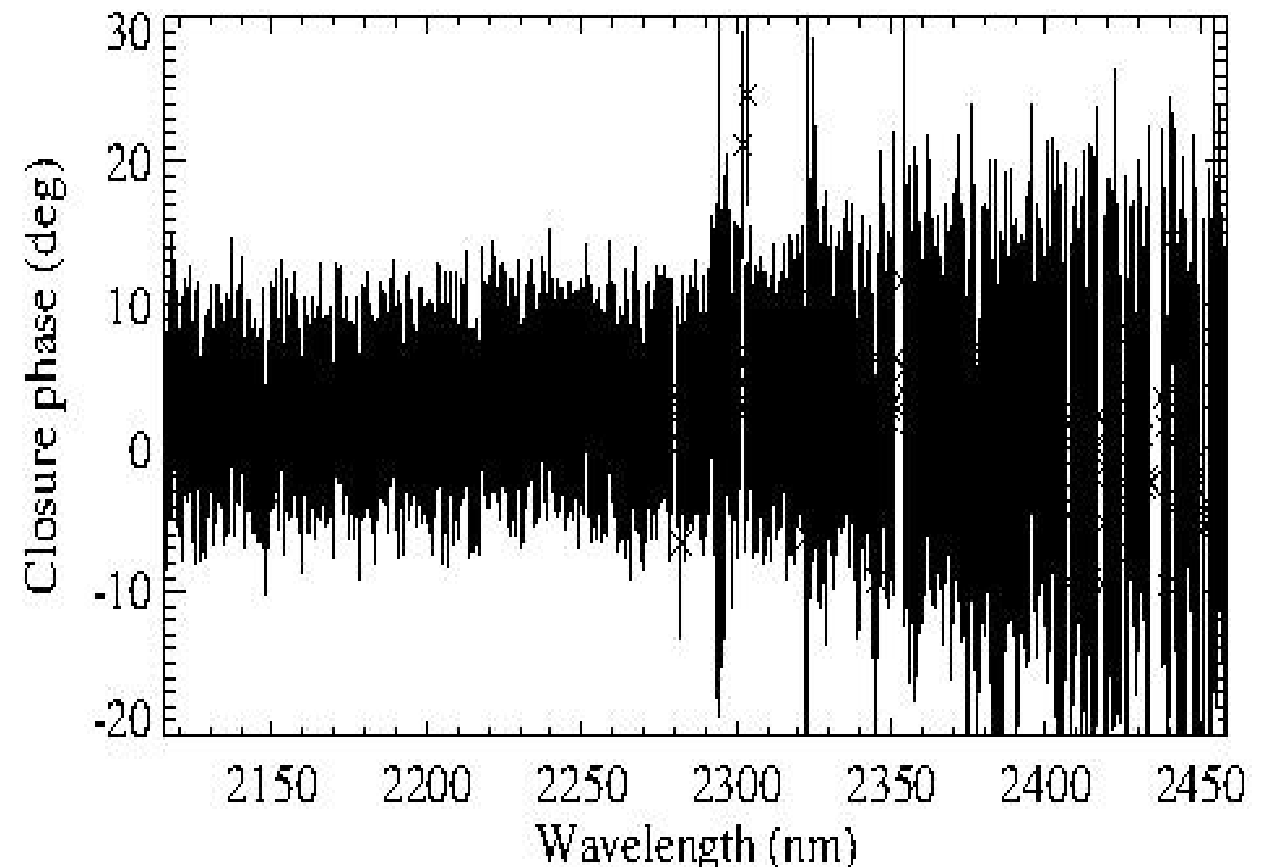


We used the models with parameters: $T_{\text{eff}}=3600$ K, $\log(g)=-0.5$ (AH Sco), $T_{\text{eff}}=3700$ K, $\log(g)=0.0$ (KW Sgr) and $T_{\text{eff}}=3400$ K, $\log(g)=-0.5$ (UYSct).

Data reduction - Results



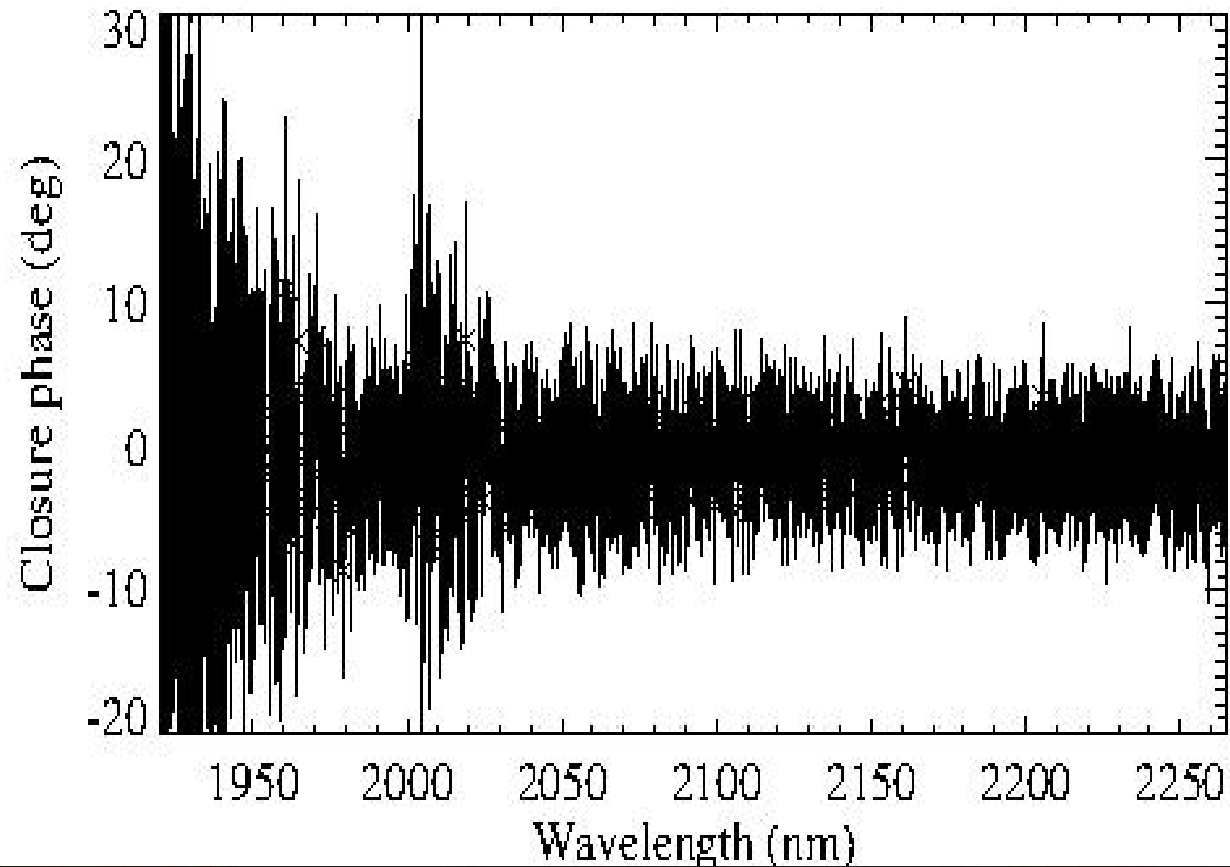
Closure Phase of AH Sco
in the K-2.1 band



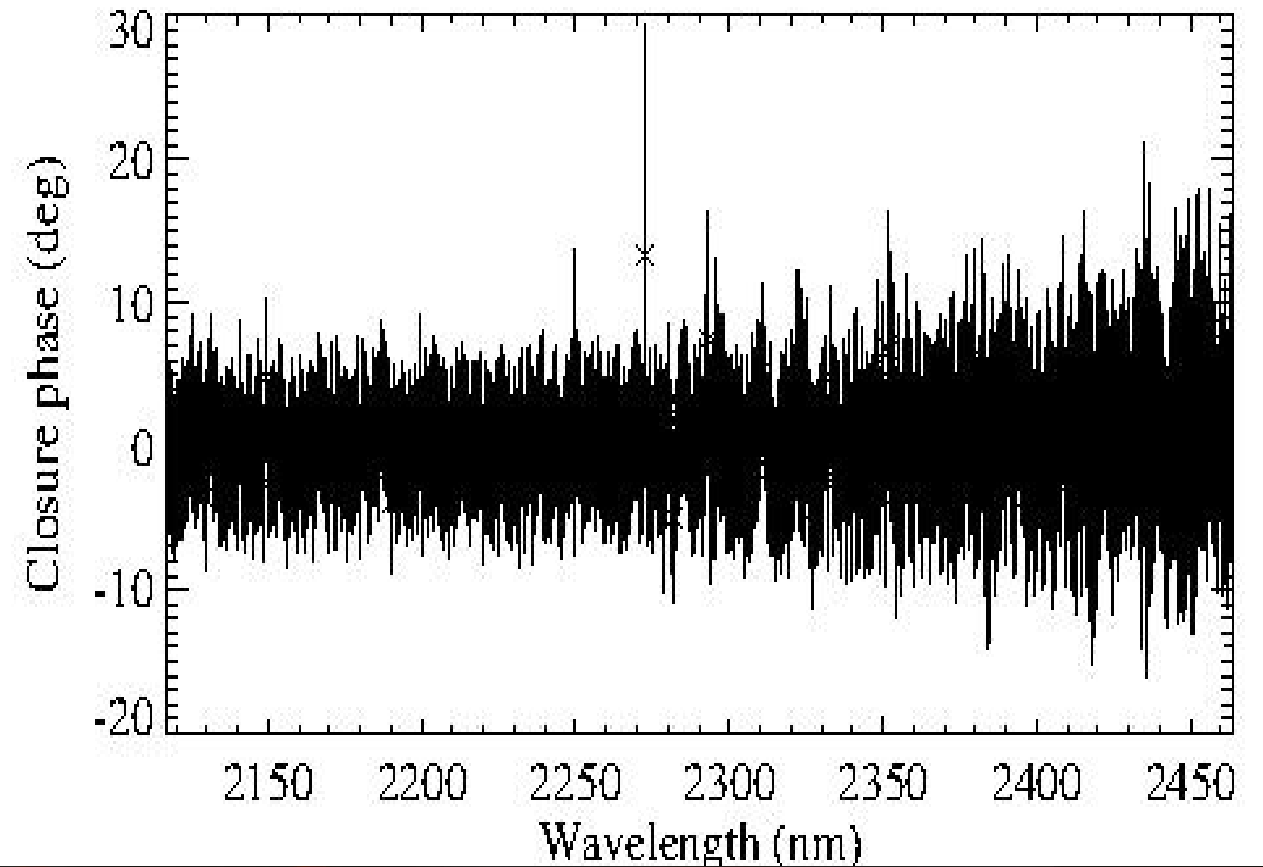
Closure Phase of AH Sco
in the K-2.3 band

The closure phase show small values of 20 deg, and do not indicate deviations from point symmetry. However, we only have data in the first lobe, so we can not exclude asymmetries at scales smaller, as observed in VY CMa.

Data reduction - Results

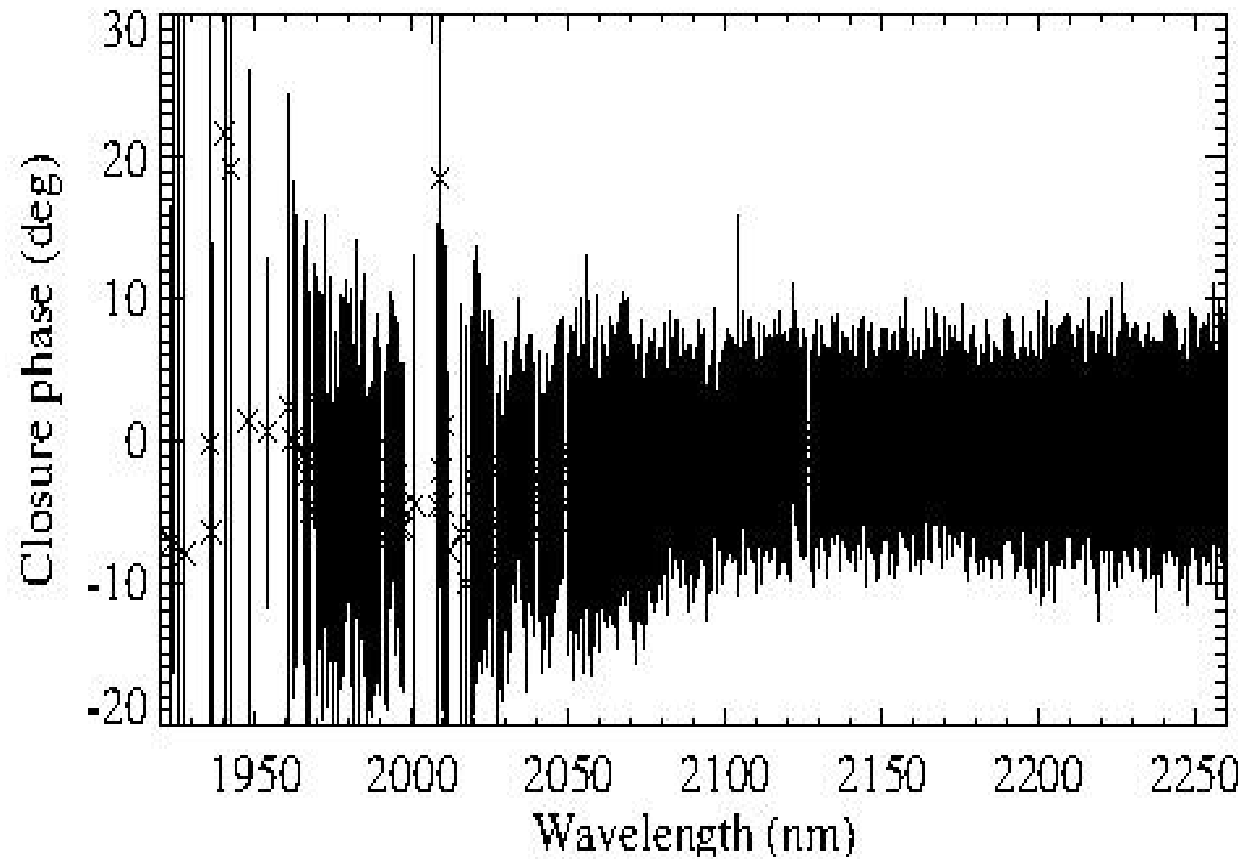


Closure Phase of KW Sgr
in the K-2.1 band

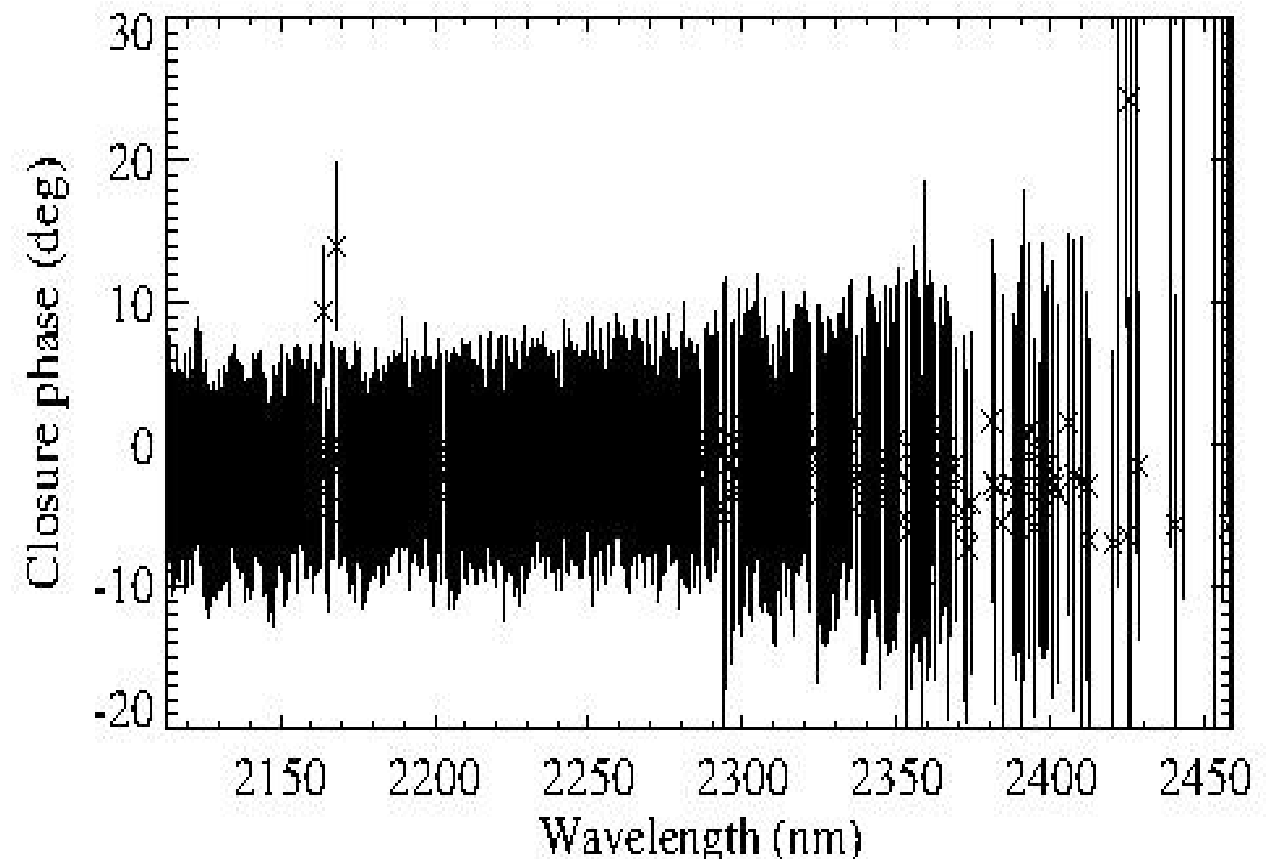


Closure Phase of KW Sgr
in the K-2.3 band

Data reduction - Results

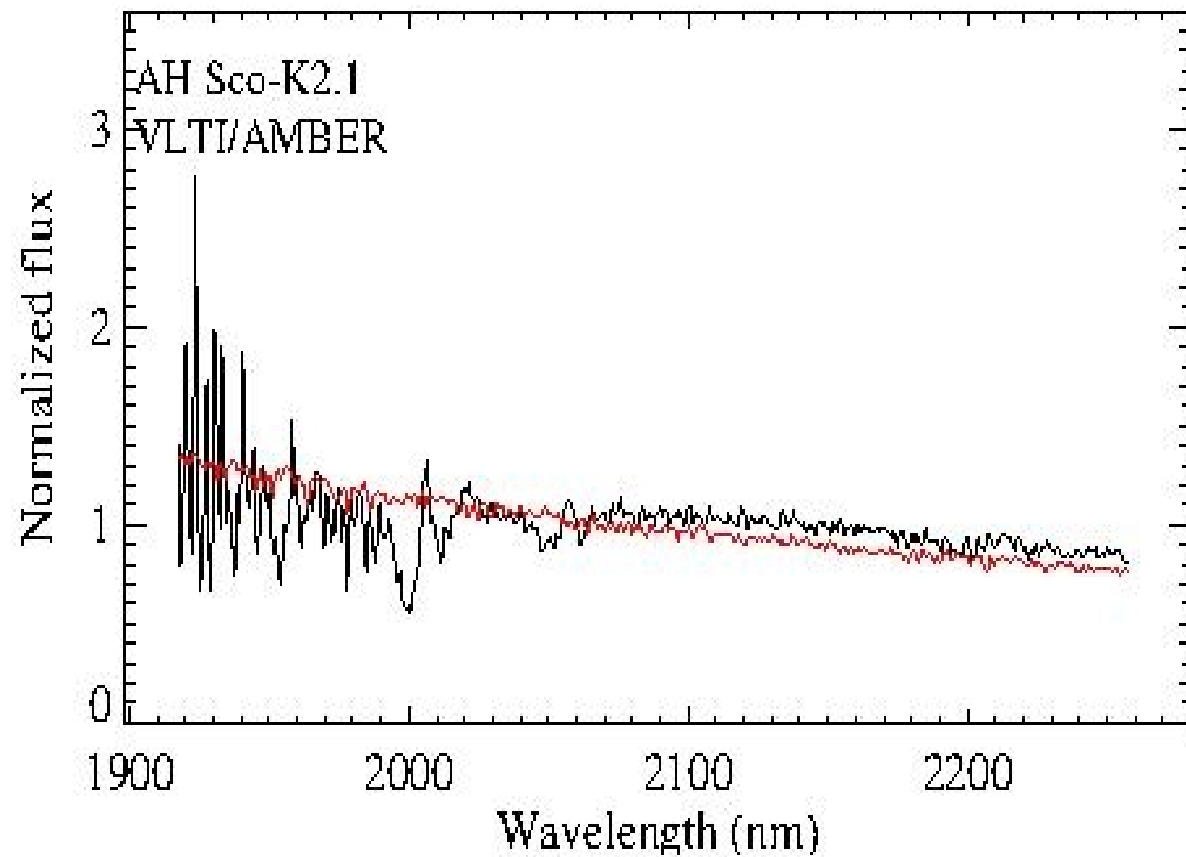


Closure Phase of UY Sct
in the K-2.1 band

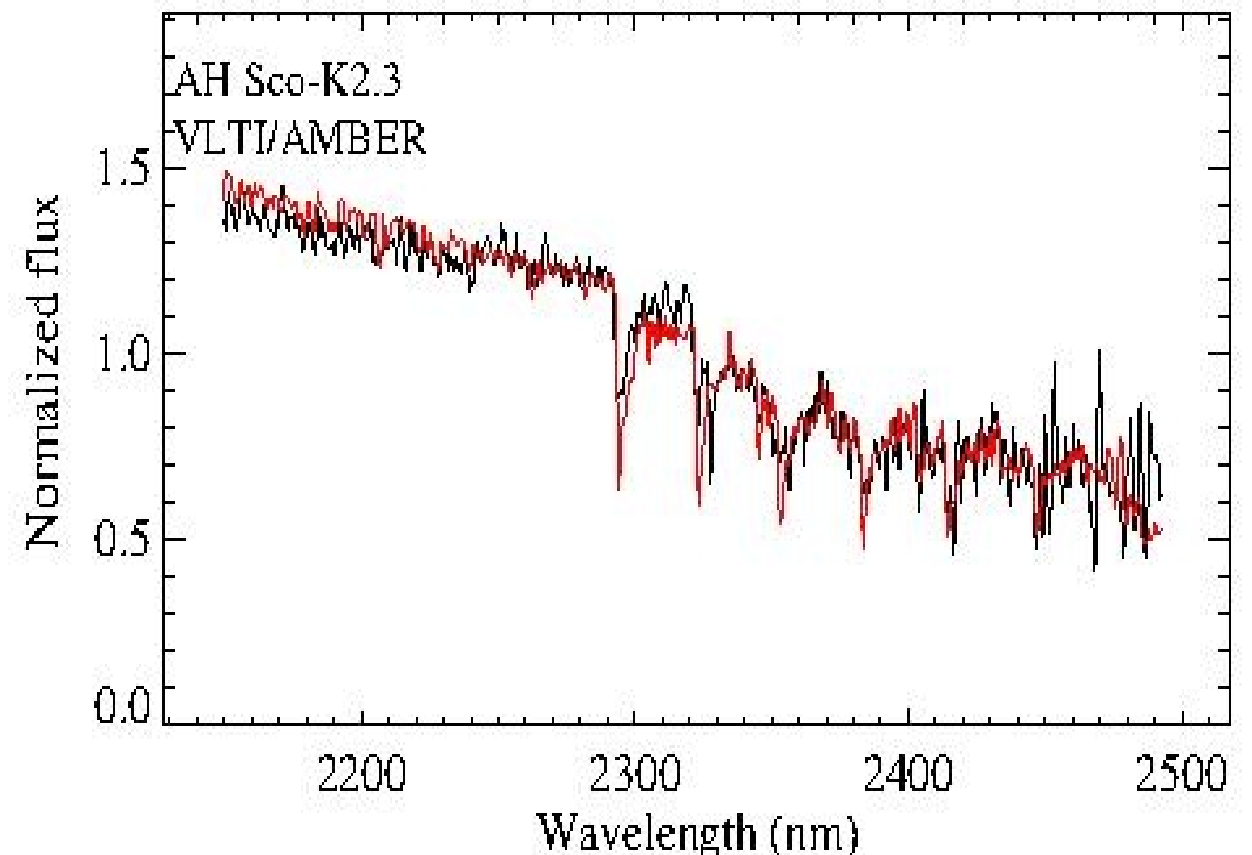


Closure Phase of UY Sct
in the K-2.3 band

Results - Normalized flux



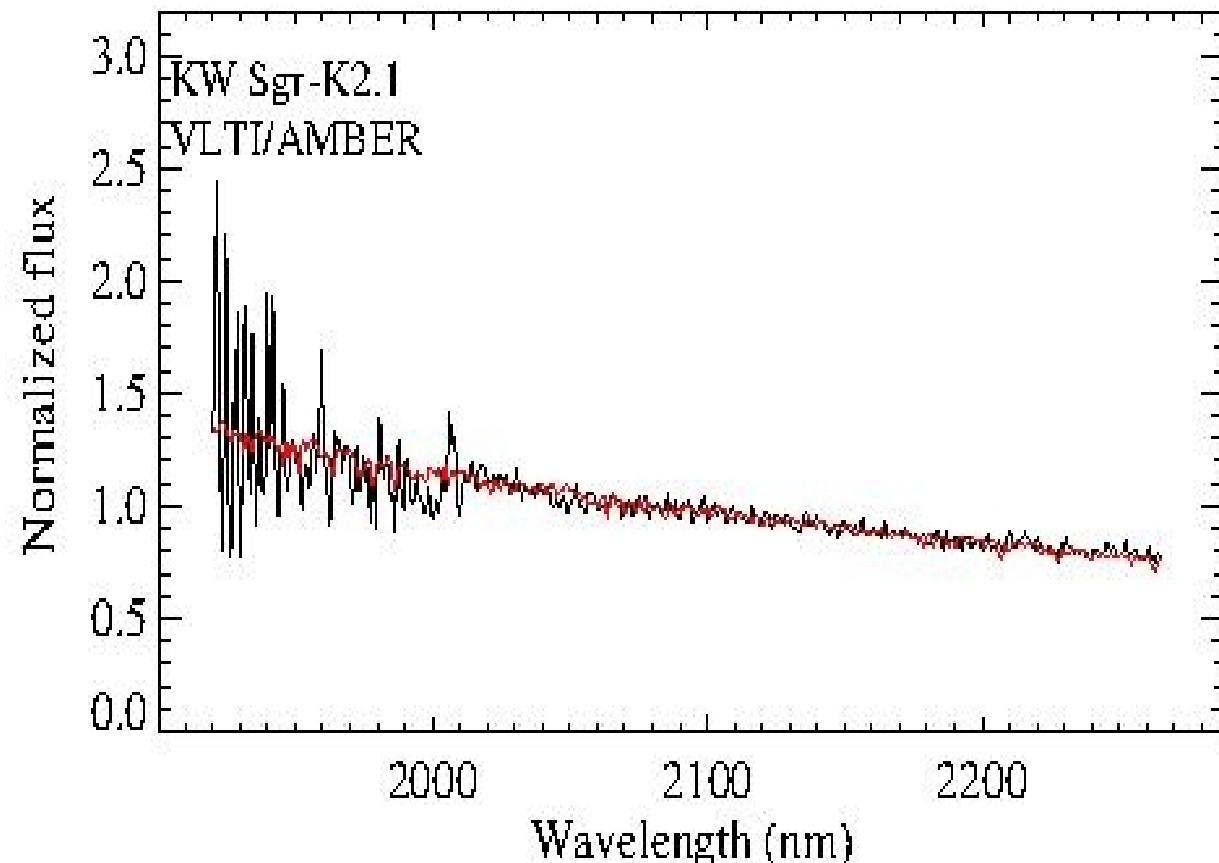
Normalized flux of AH Sco
in the K-2.1 band



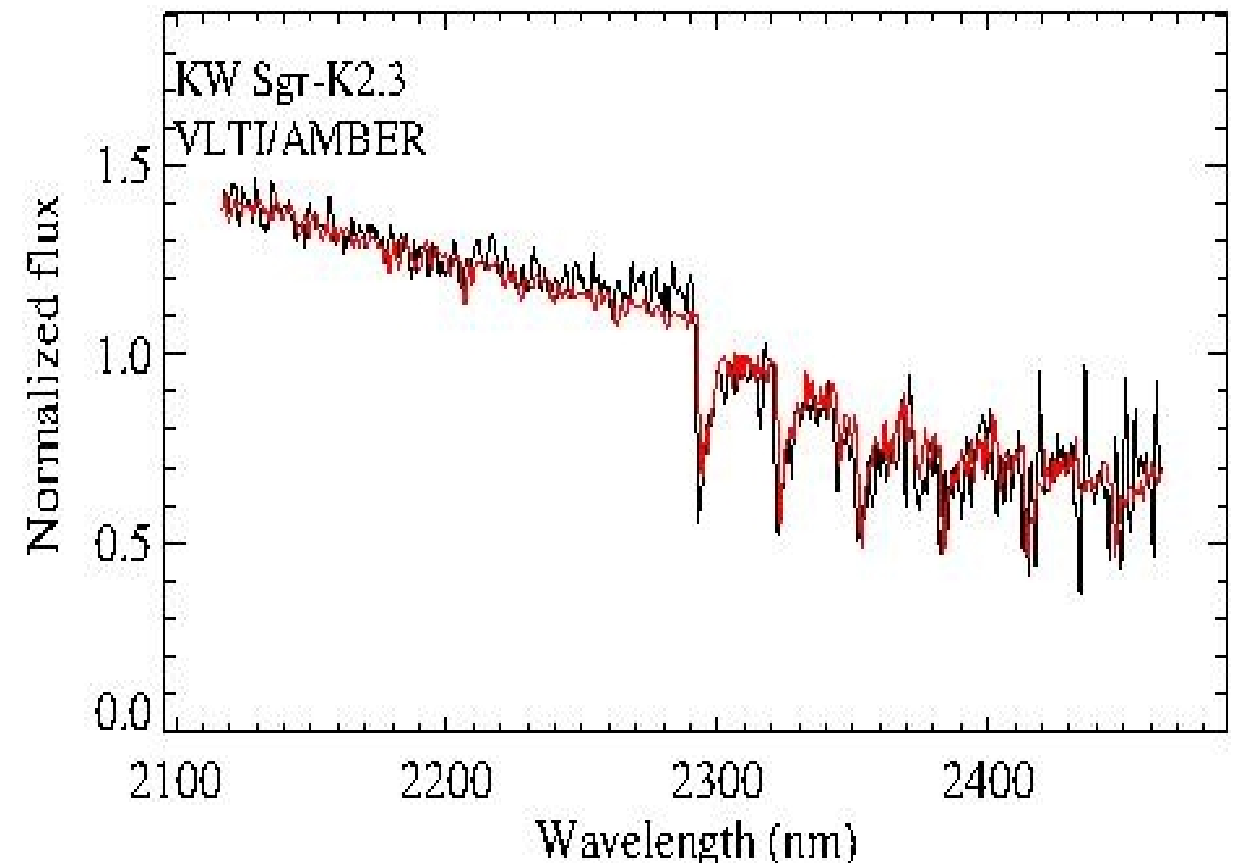
Normalized flux of AH Sco in
the K-2.3 band

Show a decreasing flux between 1.9 and 2.5 μm and exhibit strong absorption features of CO. The higher noise level at the short wavelength edge is caused by the lower instrumentation transmission.

Results - Normalized flux



Normalized flux of KW Sgr
in the K-2.1 band

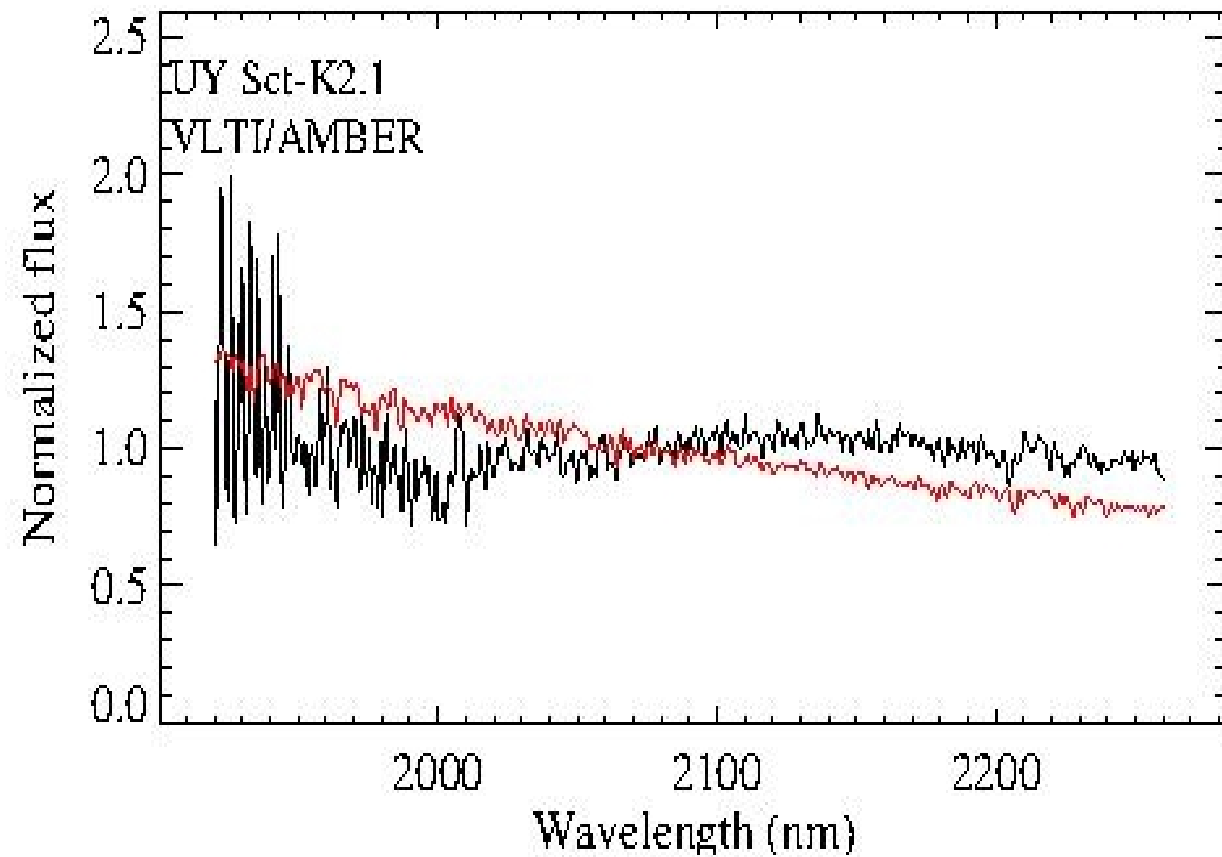


Normalized flux of KW Sgr
in the K-2.3 band

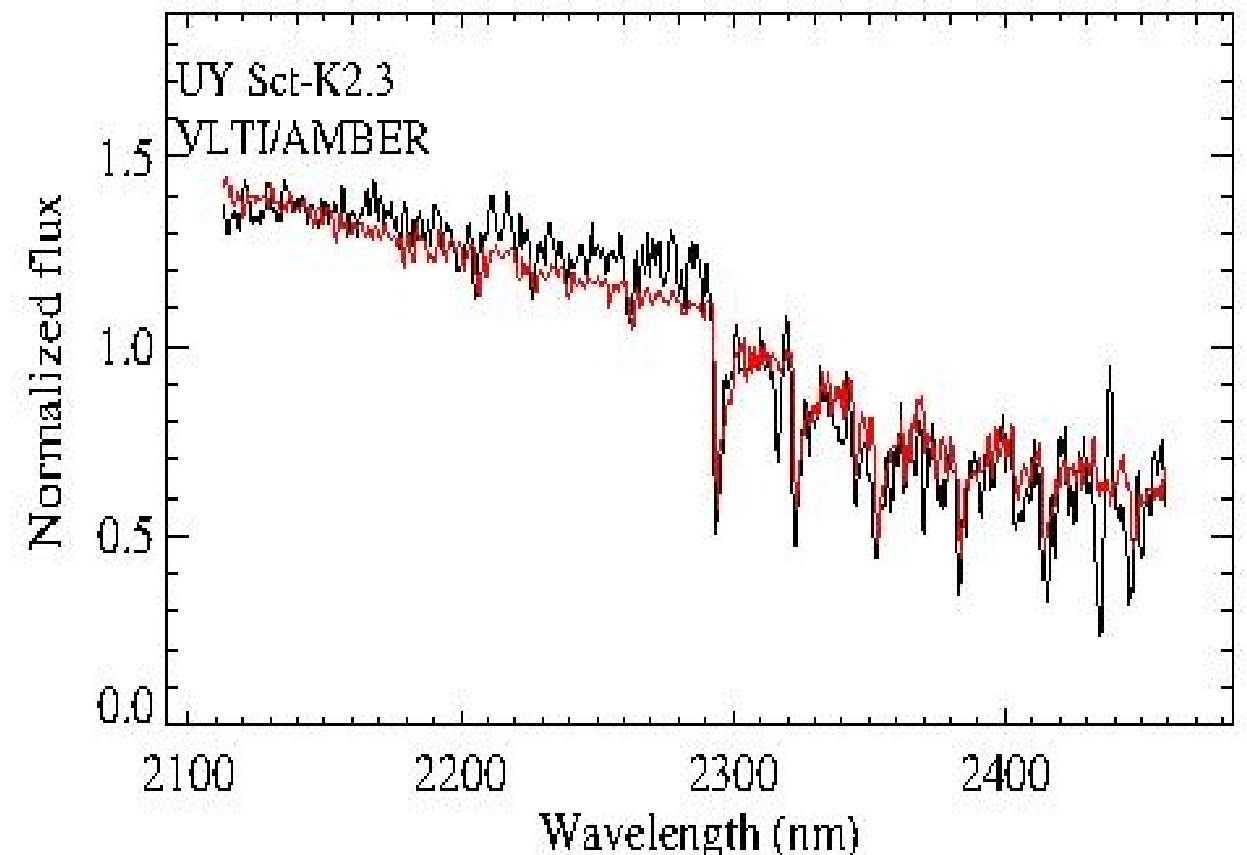
✦ Fit to synthetic spectra:

Near-infrared spectra are predicted reasonably well by static PHOENIX model atmospheres.

Results - Normalized flux



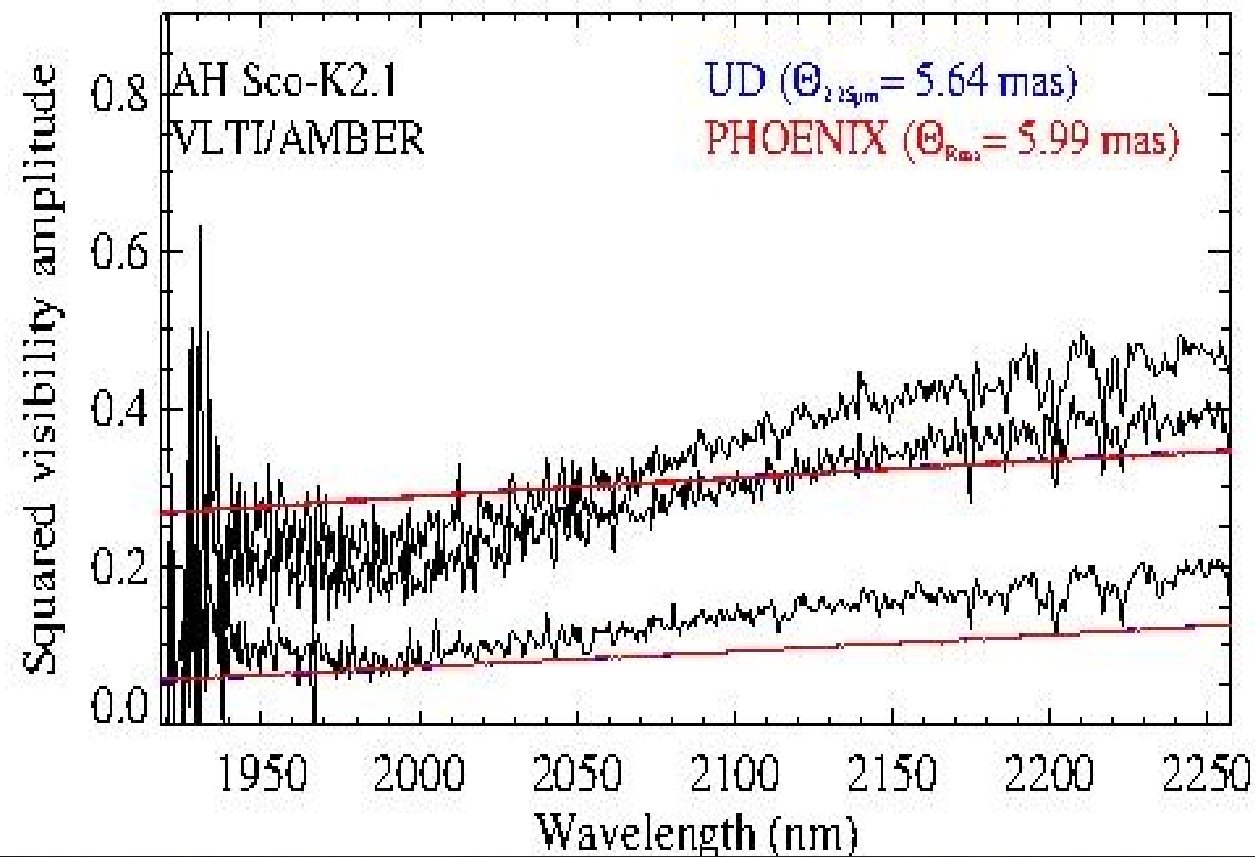
Normalized flux of UY Sct
in the K-2.1 band



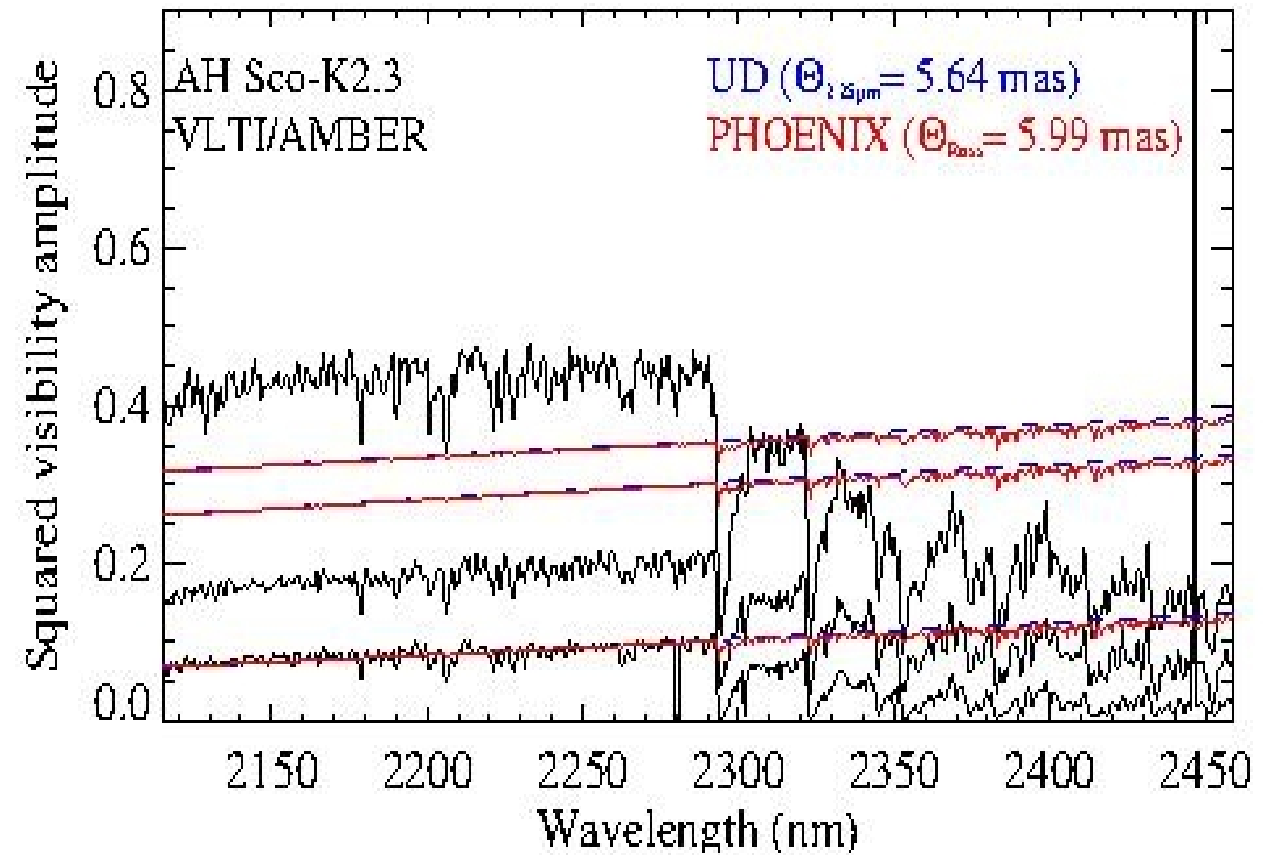
Normalized flux of UY Sct
in the K-2.3 band

For the cooler stars, as UY Sct, we observe discrepancies in the water band (water layer that are no included in the model).

Results - Square amplitude visibility



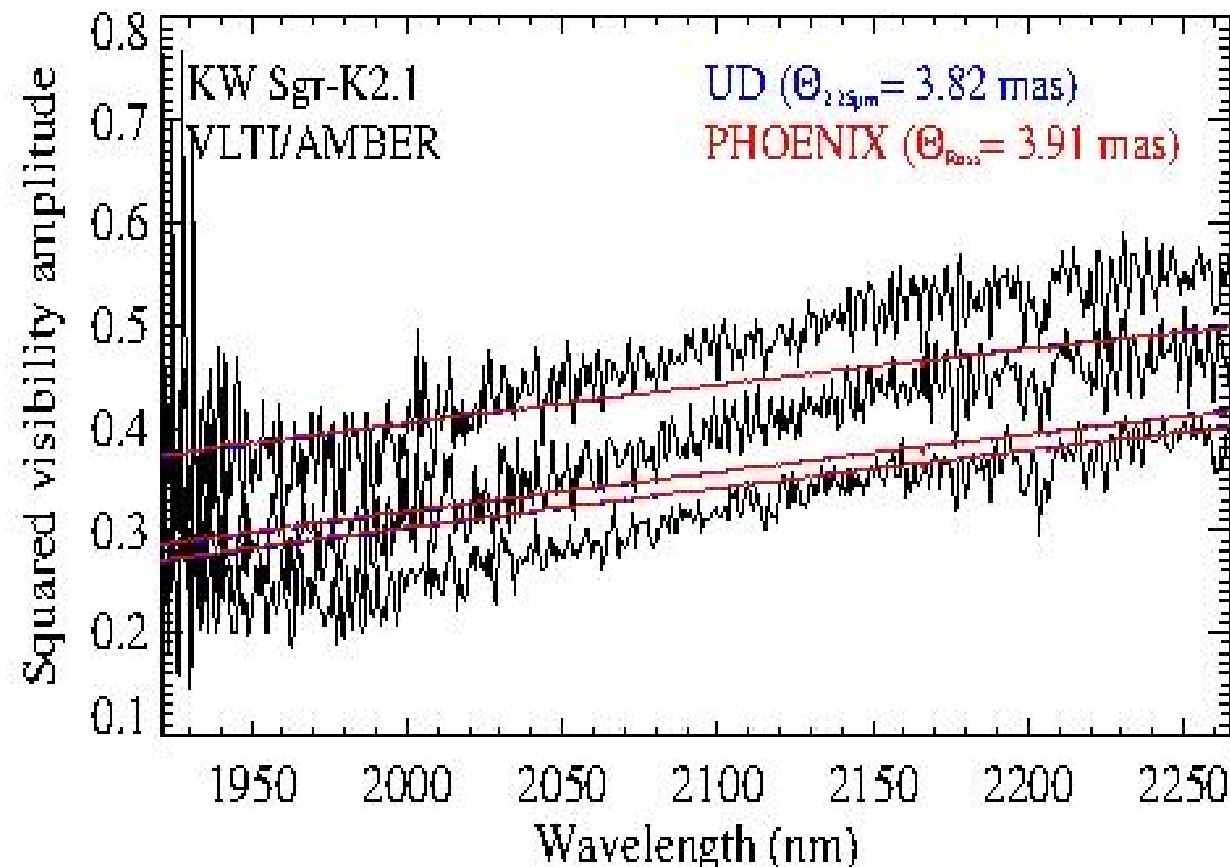
Squared visibility of AH Sco
in the K-2.1 band



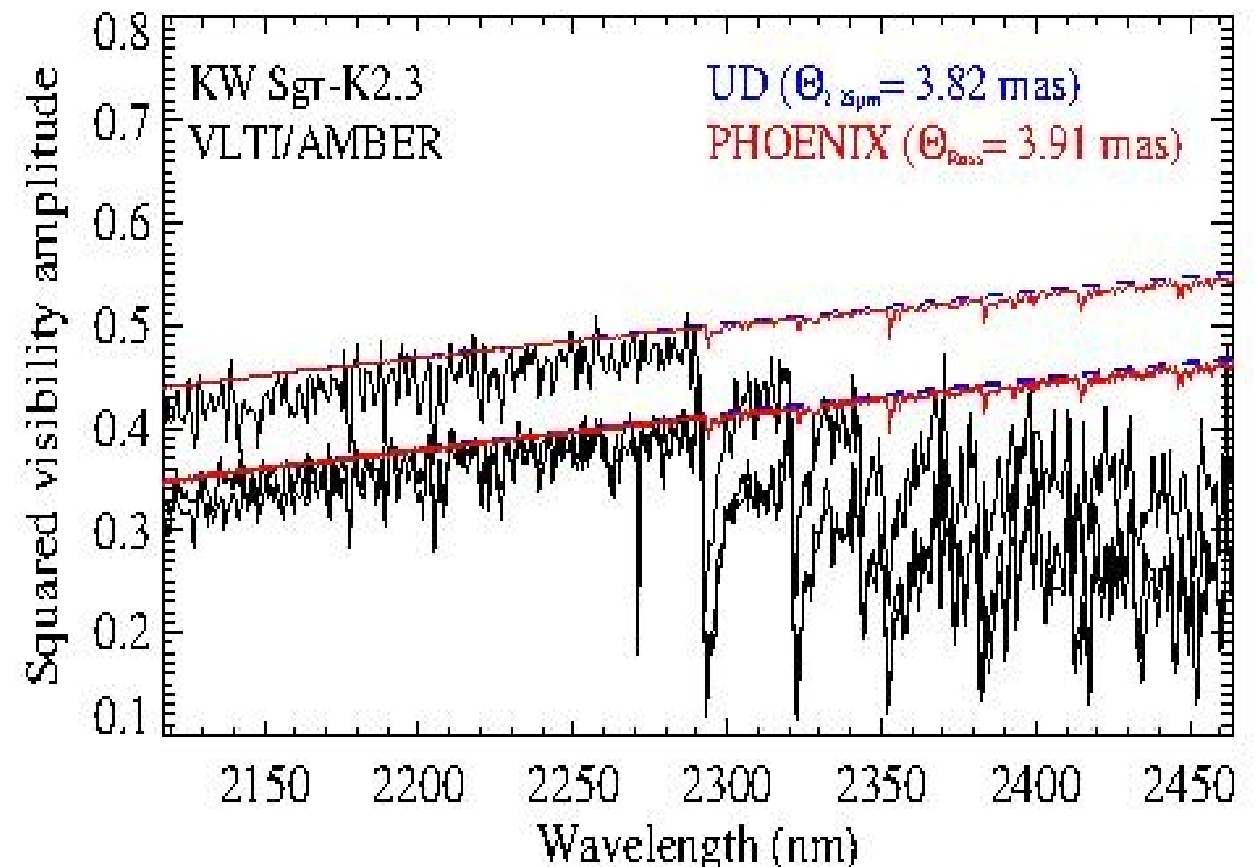
Squared visibility of AH Sco
in the K-2.3 band

Show a maximum near $2.25 \mu\text{m}$, and a decrease towards the water bands (centered at $1.9 \mu\text{m}$) and at positions of the CO bands.

Results - Square amplitude visibility



Squared visibility of KW Sgr
in the K-2.1 band

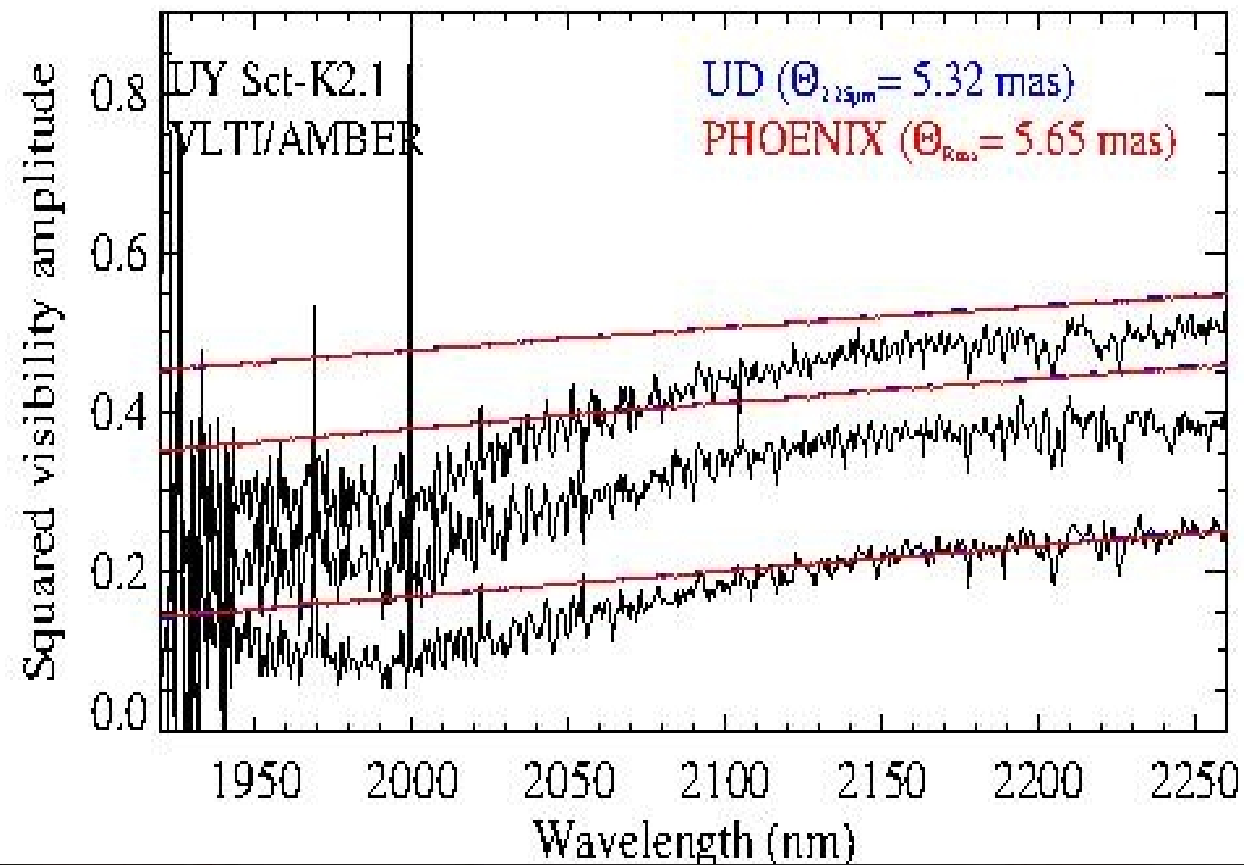


Squared visibility of KW Sgr
in the K-2.3 band

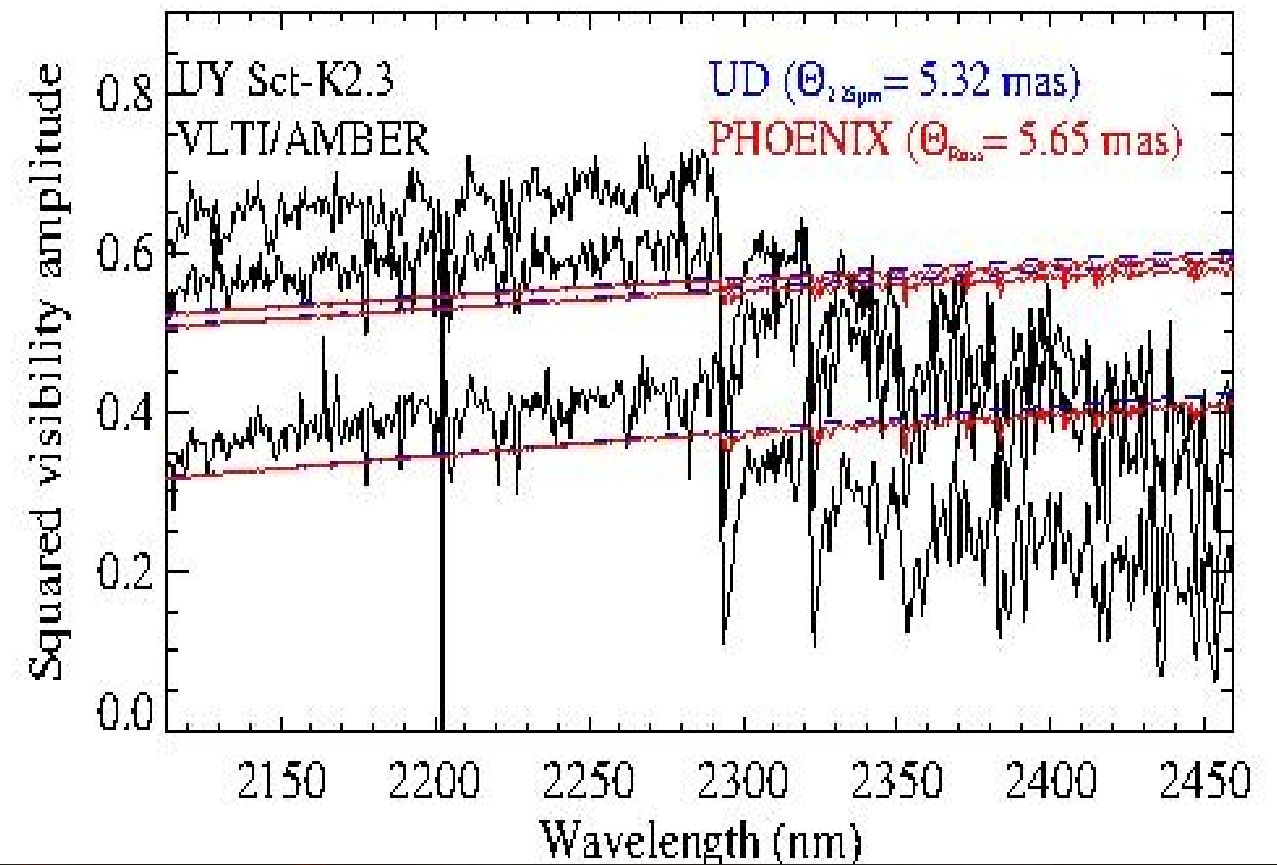
✘ Fit to synthetic visibilities:

The CO and water bands are not reproduced by the PHOENIX model atmospheres. The synthetic visibility show features at the location of these CO bands, but which are much weaker compared to the observed data. The water bands are not visible in the model visibility.

Results - Square amplitude visibility

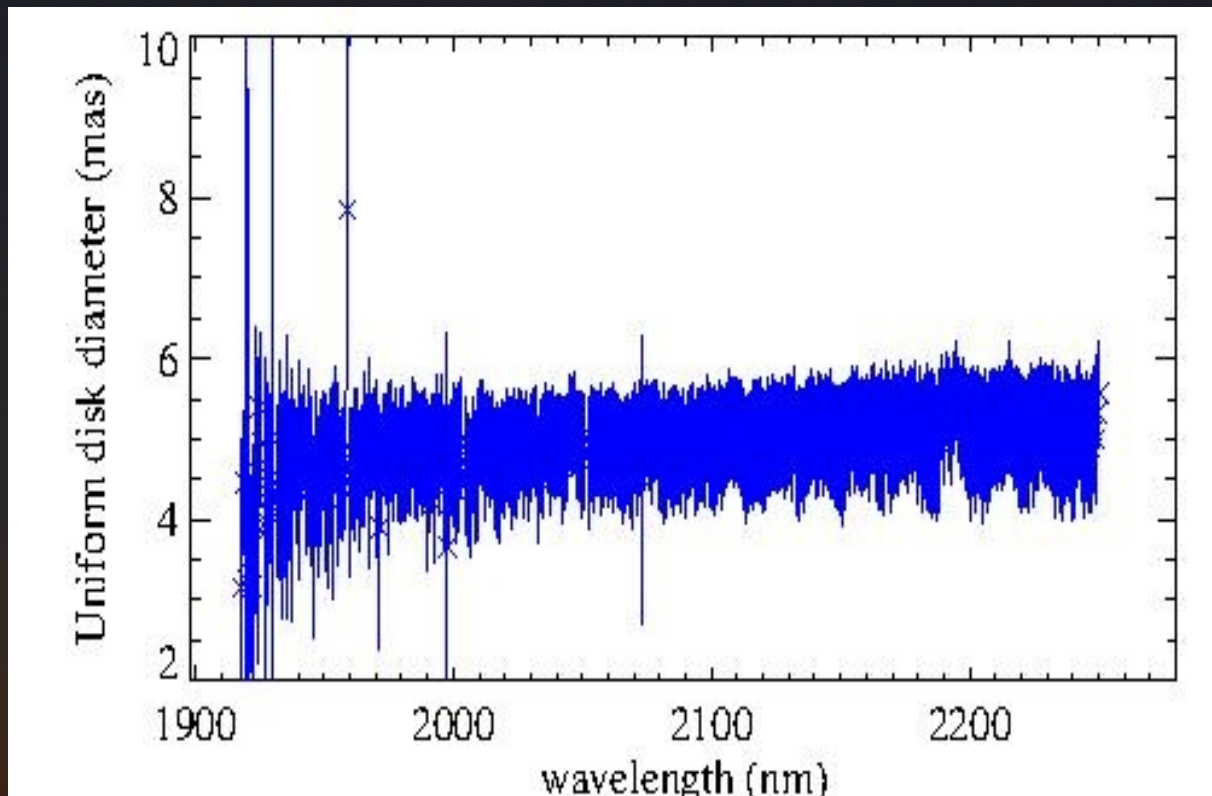


Squared visibility of UY Sct
in the K-2.1 band

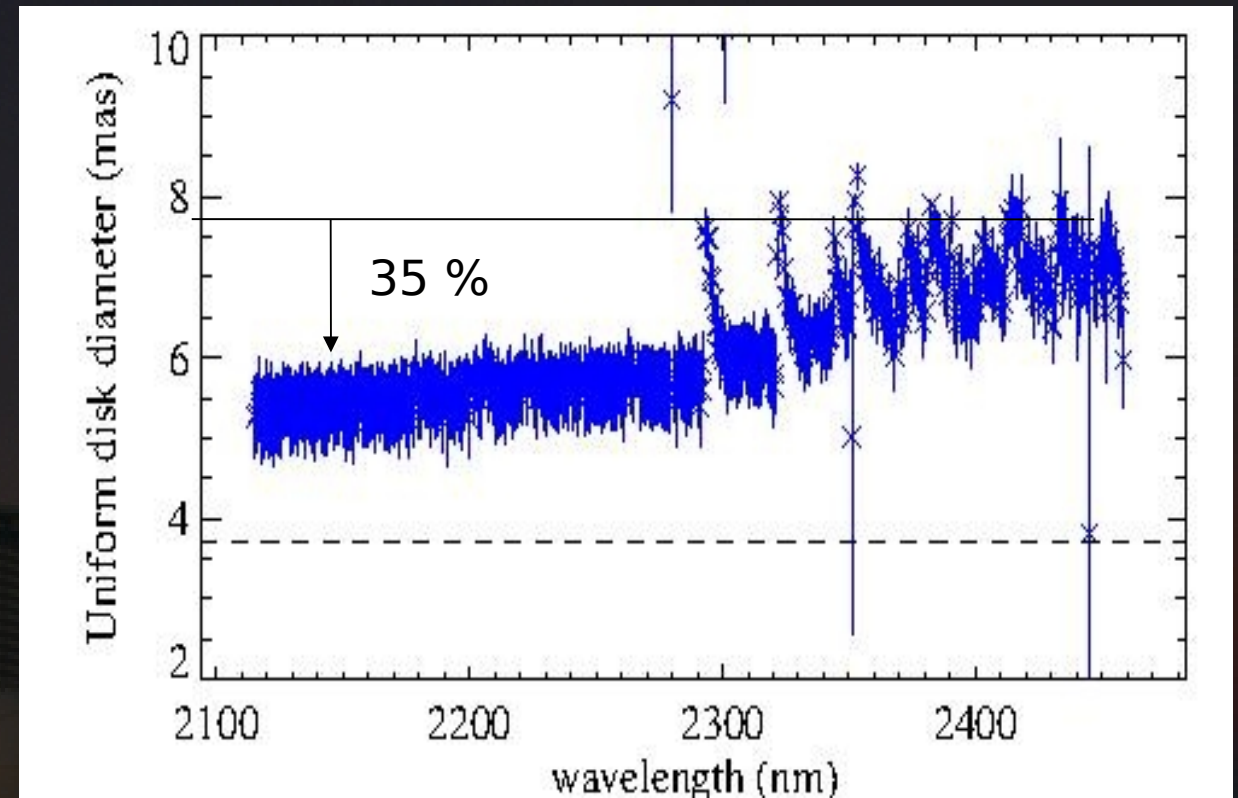


Squared visibility of UY Sct
in the K-2.3 band

Results – UD diameter



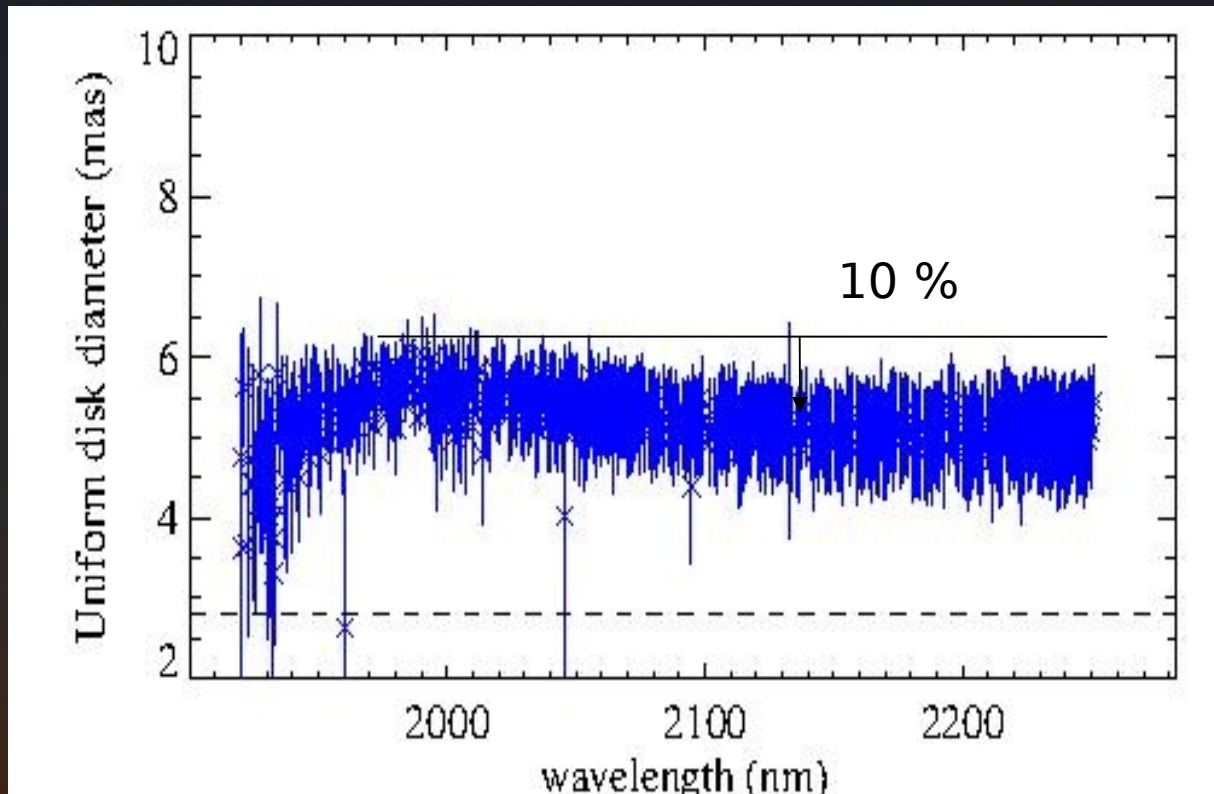
UD diameter of AH Sco in the K-2.1 band



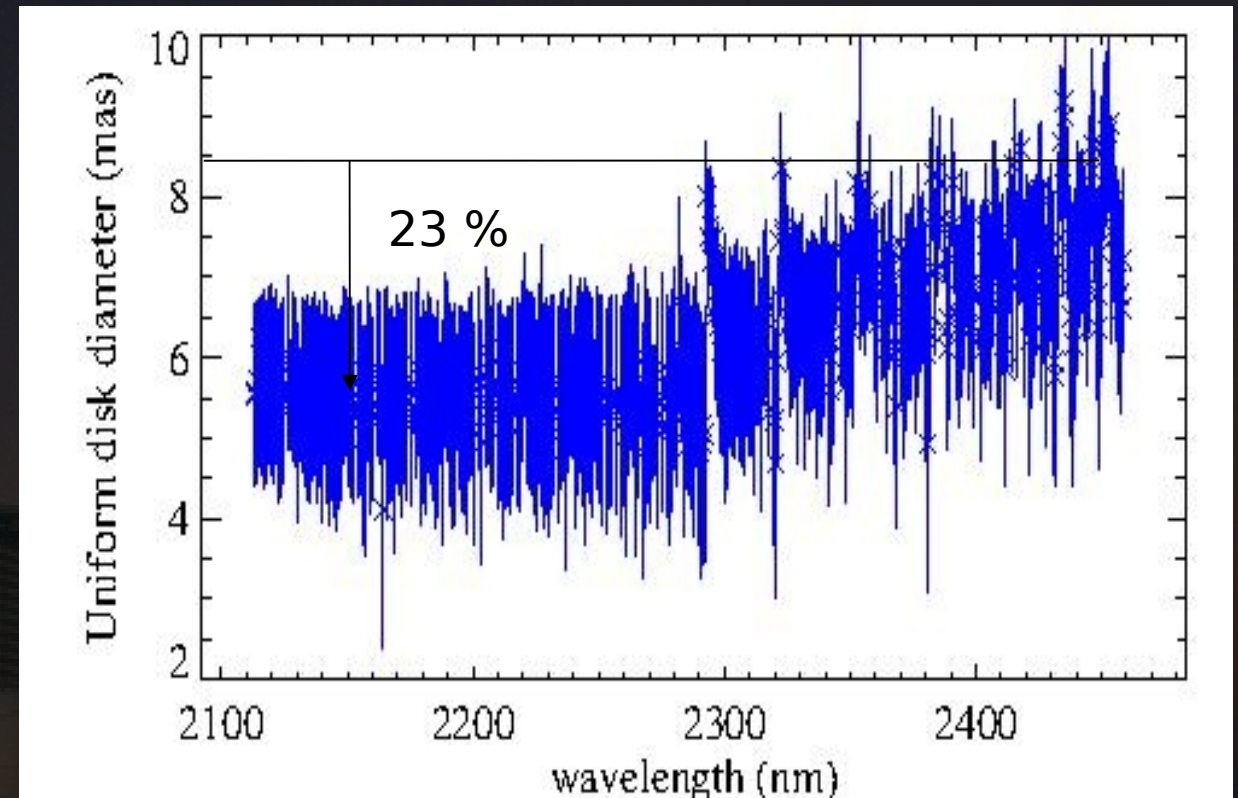
UD diameter of AH Sco in the K-2.3 band

Exhibit a minimum with a constant diameter in the continuum (2.20-2.25 μm), and it increases in the CO and water bands.

Results – UD diameter

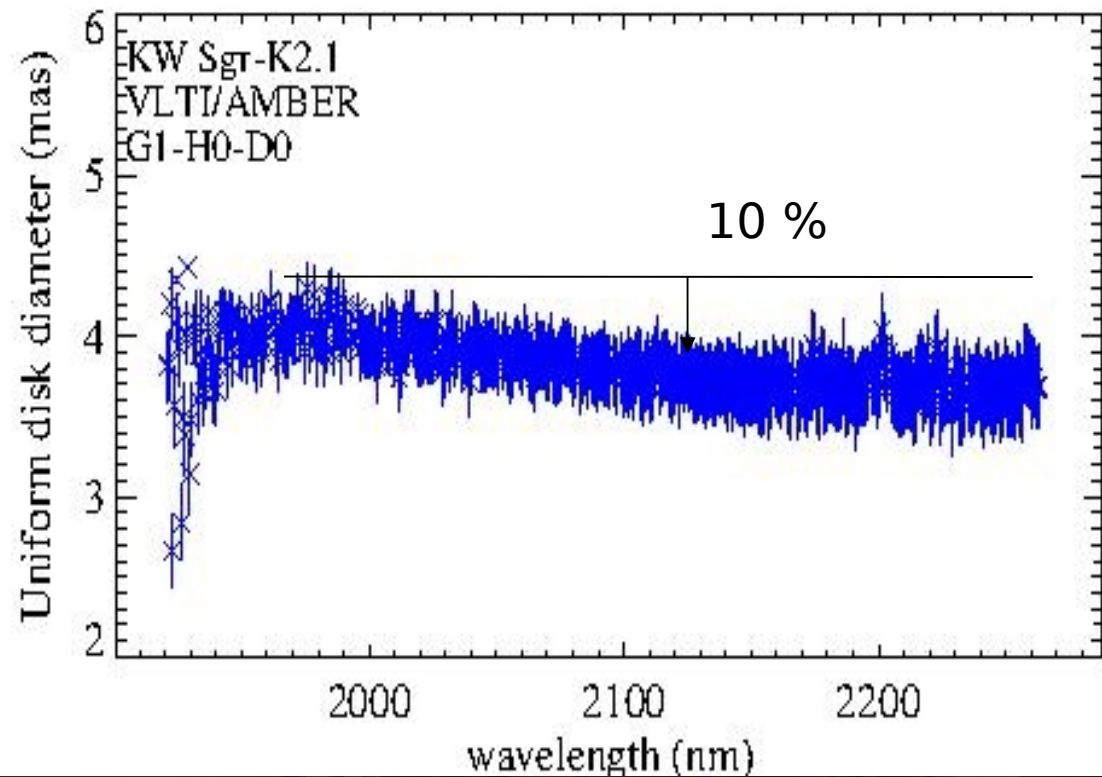


UD diameter of UY Sct
in the K-2.1 band

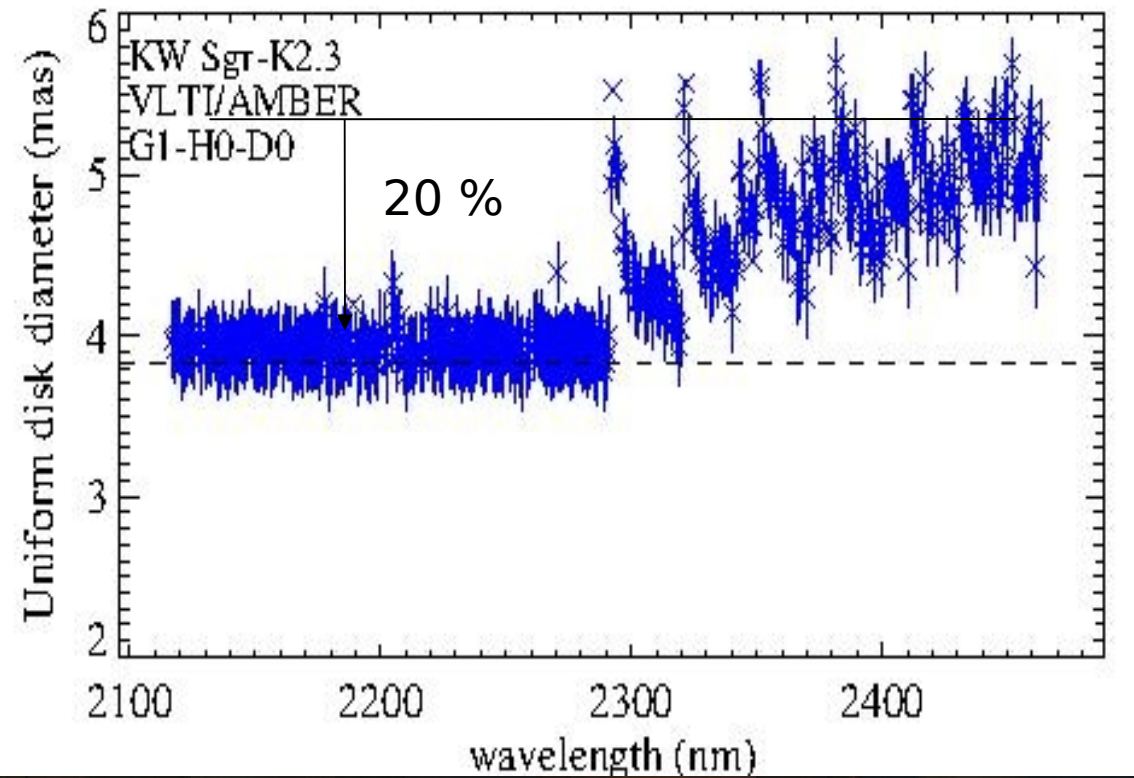


UD diameter of UY Sct
in the K-2.3 band

Results – UD diameter

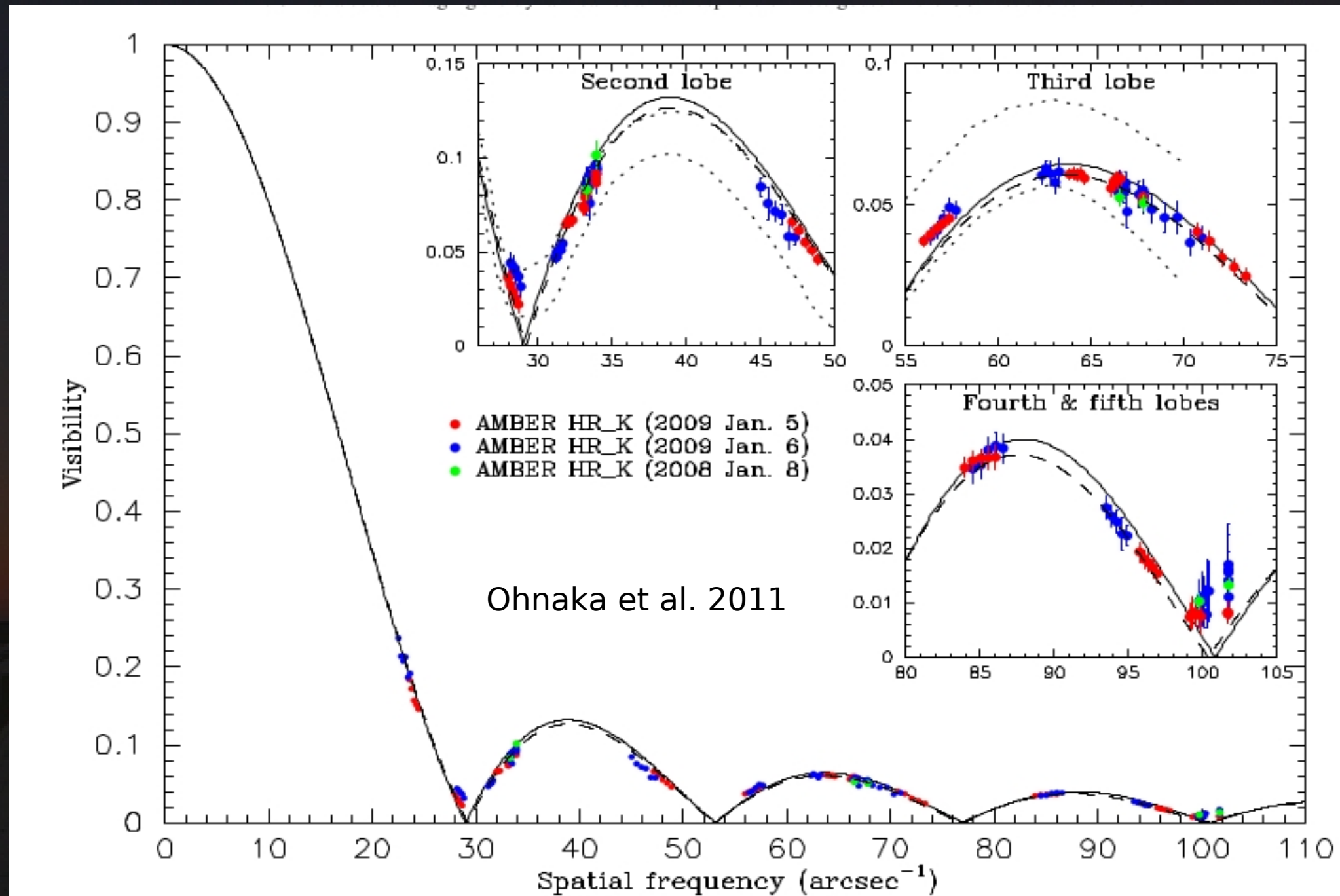


UD diameter of KW Sgr
in the K-2.1 band



UD diameter of KW Sgr
in the K-2.3 band

Fit in the continuum



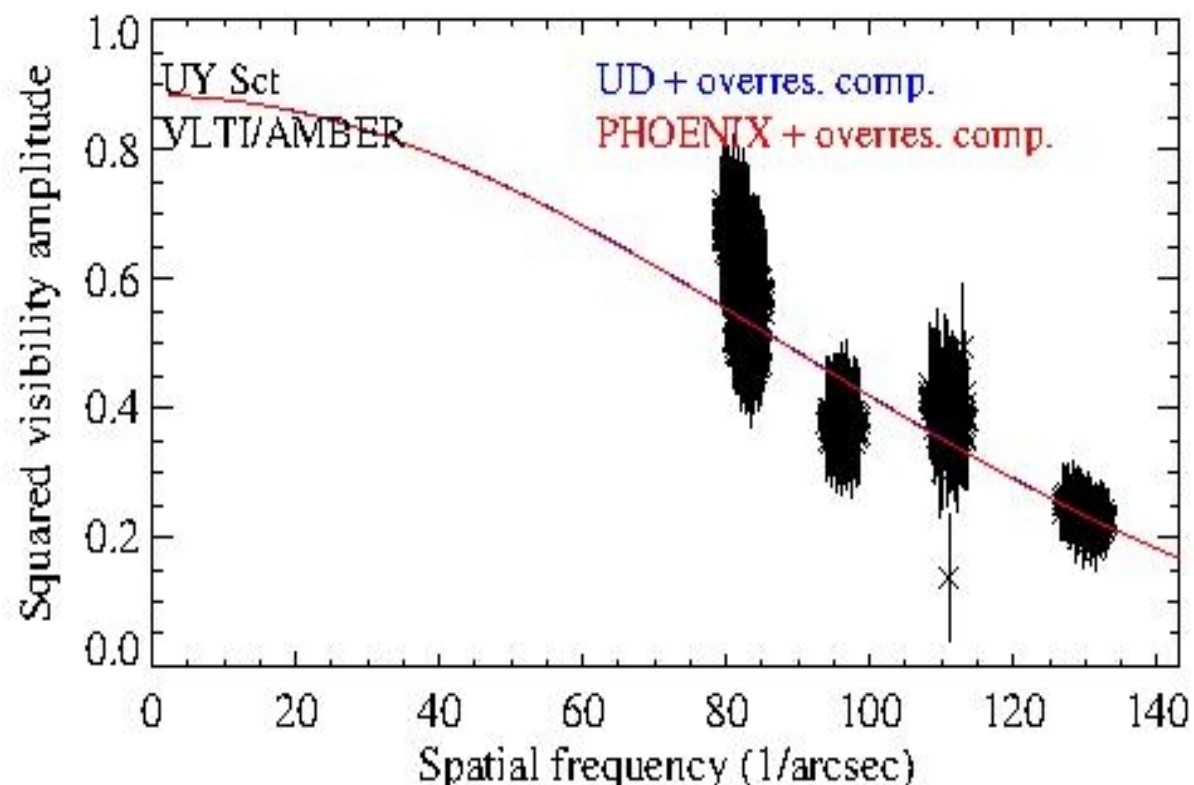
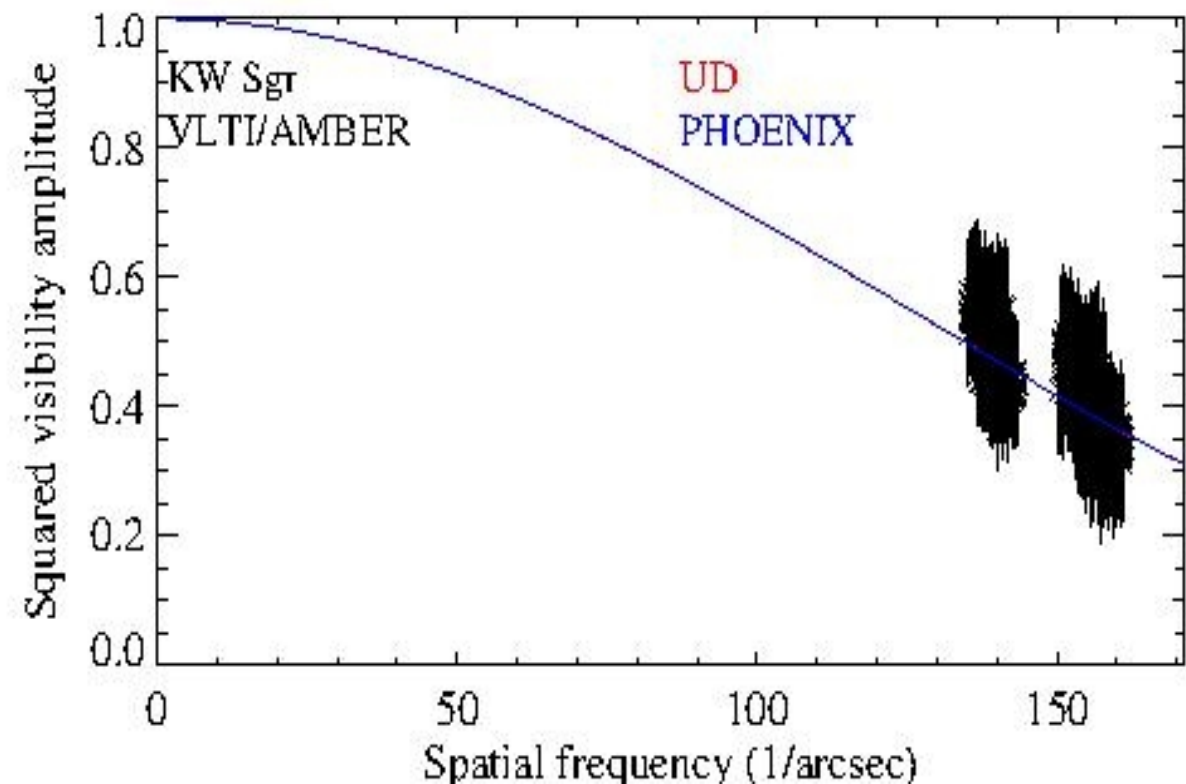
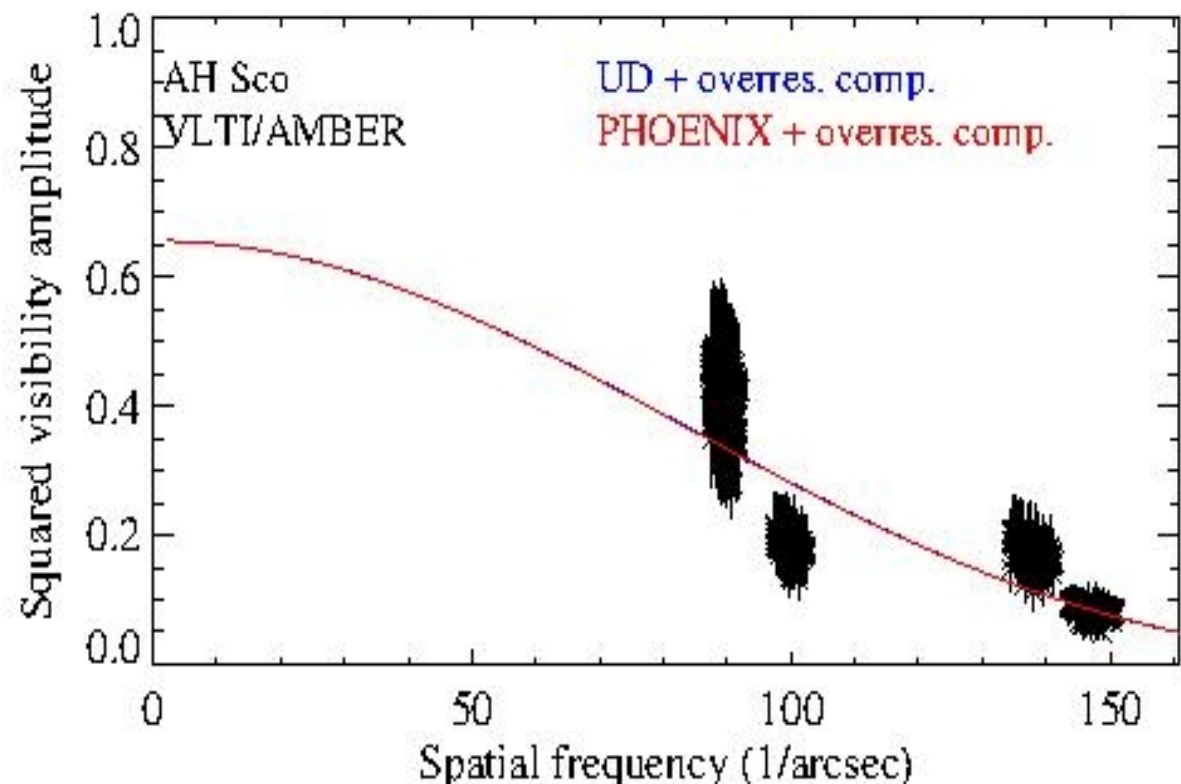
Interferometric observations of RSGs at continuum band-passes showed that the photosphere can be well described by a limb-darkened disk (Perrin et al. 2004, Ohnaka et al, 2011)

Results - Angular diameter

	AH Sco	KW Sgr	UY Sct	Betelgeuse
θ_{Ross}	5.99 ± 0.15	3.91 ± 0.25	$5,66 \pm 0.1$	43.20 ± 0.2
S	0.81	1.00	0.94	1.00

* Results obtained from the archival Betelgeuse data (we reduce this data)

Results - Visibility vs. spatial frequency



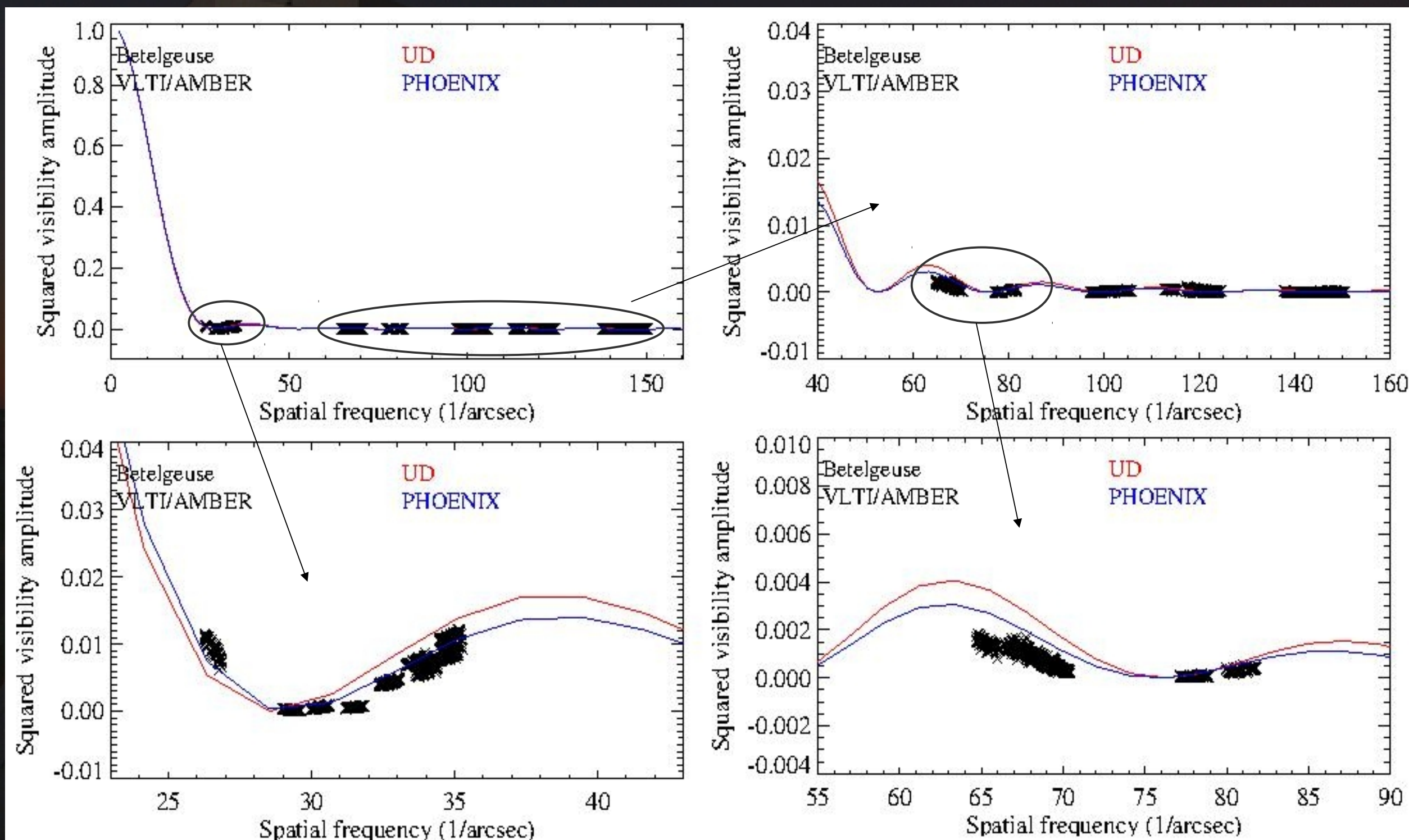
Visibility data of the near-continuum bandpass.

fit to...

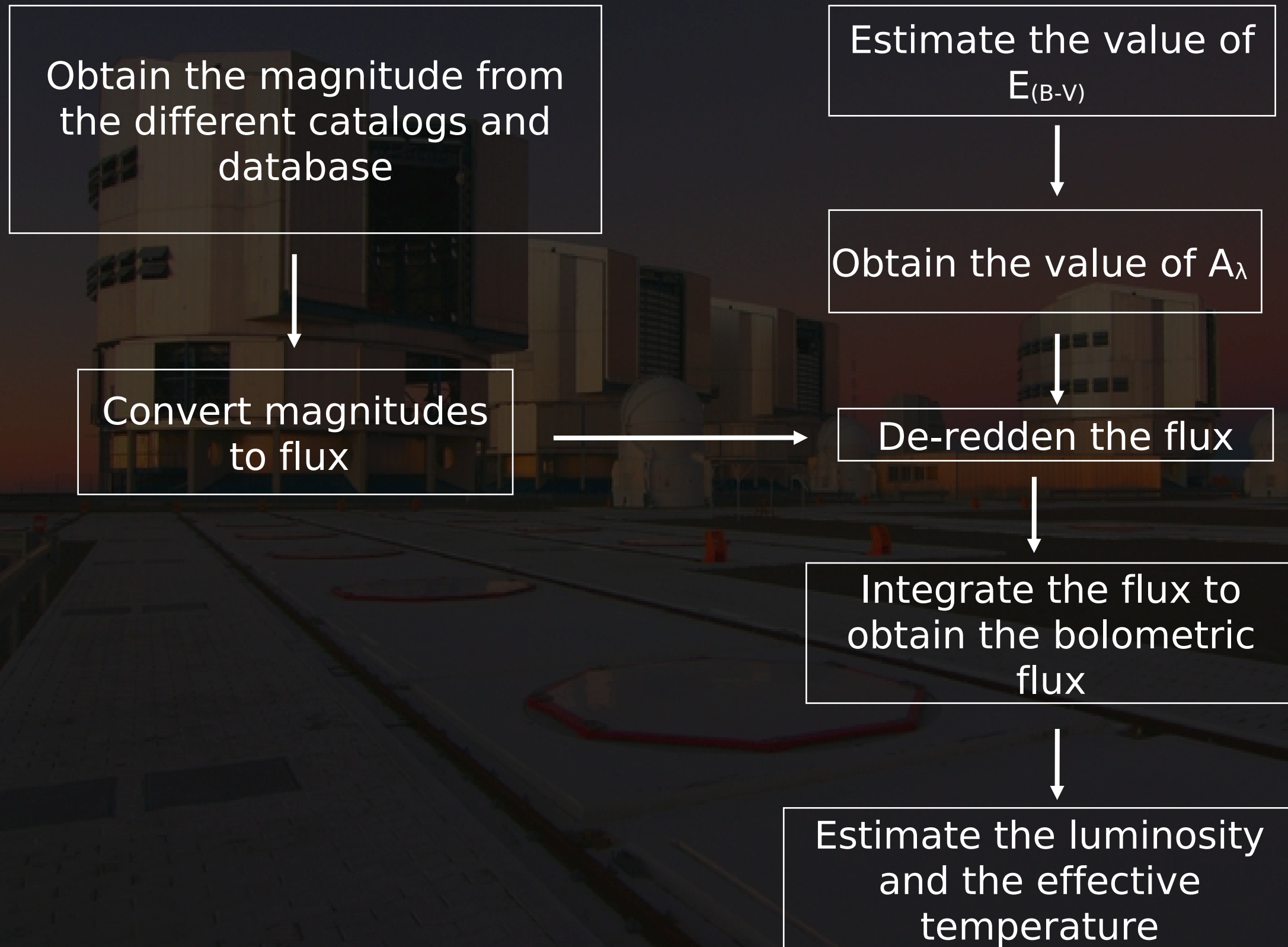
A UD and PHOENIX atmospheric models

Results - Visibility vs. spatial frequency

Our results of archival Betelgeuse data...



Fundamental parameters



Fundamental parameters

	AH Sco	UY Sct	KW Sgr	Reference
$F_{\text{bol}} (10^{-9} \text{ W m}^{-2})$	2.07 ± 0.21	1.28 ± 0.3	0.97 ± 0.097	Estimated in this work using the magnitudes from catalogs
$d \text{ (pc)}$	$2260 \pm 190 \text{ (1)}$	$2900 \pm 317 \text{ (2)}$	$2400 \pm 300 \text{ (3)}$	(1) Chen, X., Shen, Z.-Q. (2008) (2) Sylvert, C. J. et al. (1998) (3) Melnik, A. M., Dambis, A. K., (2009)
$L (10^{32} \text{ W})$	126 ± 0.25	1.29 ± 0.30	0.67 ± 0.18	Estimated in this work
$\log(L/L_{\text{sun}})$	$5,52 \pm 0.20$	$5,53 \pm 0.24$	$5,24 \pm 0.27$	Estimated in this work
$\theta_{\text{Ross}} \text{ (mas)}$	5.99 ± 0.15	5.65 ± 0.10	43.91 ± 0.25	Estimated in this work
$T_{\text{eff}} \text{ (K)}$	3626 ± 104	3213 ± 96	3720 ± 151	Estimated in this work
$\log(T_{\text{eff}})$	$3,56 \pm 0.03$	$3,52 \pm 0.03$	$3,52 \pm 0.03$	Estimated in this work
$R(R_{\text{sun}})$	1455 ± 251	1761 ± 243	1009 ± 213	Estimated in this work

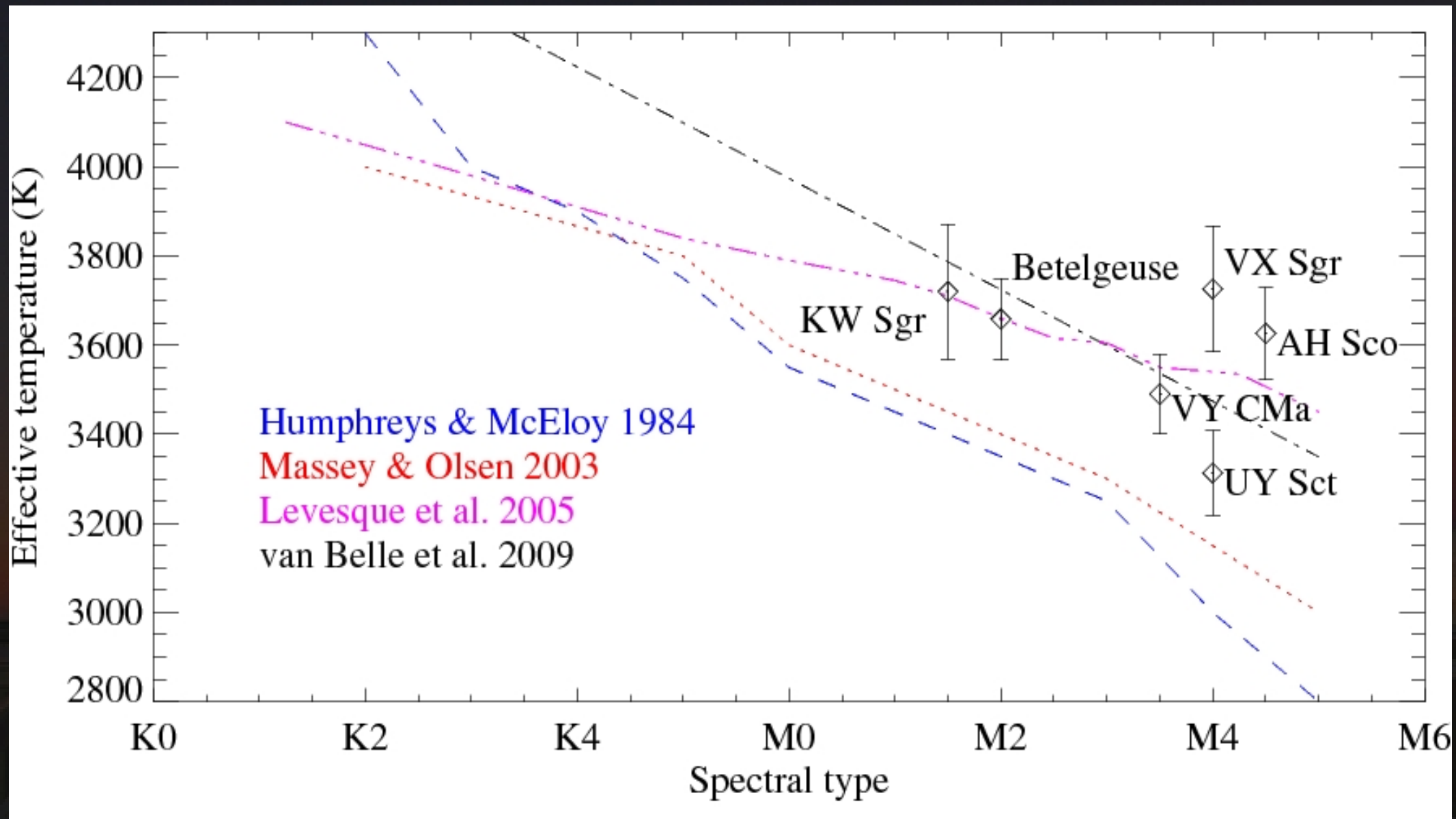
Fundamental parameters

We add three sources observed in a similar way using the VLT/AMBER instrument for compared with our targets: Betelgeuse (Kervella et al. 2009, 2011), VX Sgr (Chiavassa et al. 2010) and VY CMa (Wittkowski et al. 2012)

We calculated the effective temperature and luminosity using....

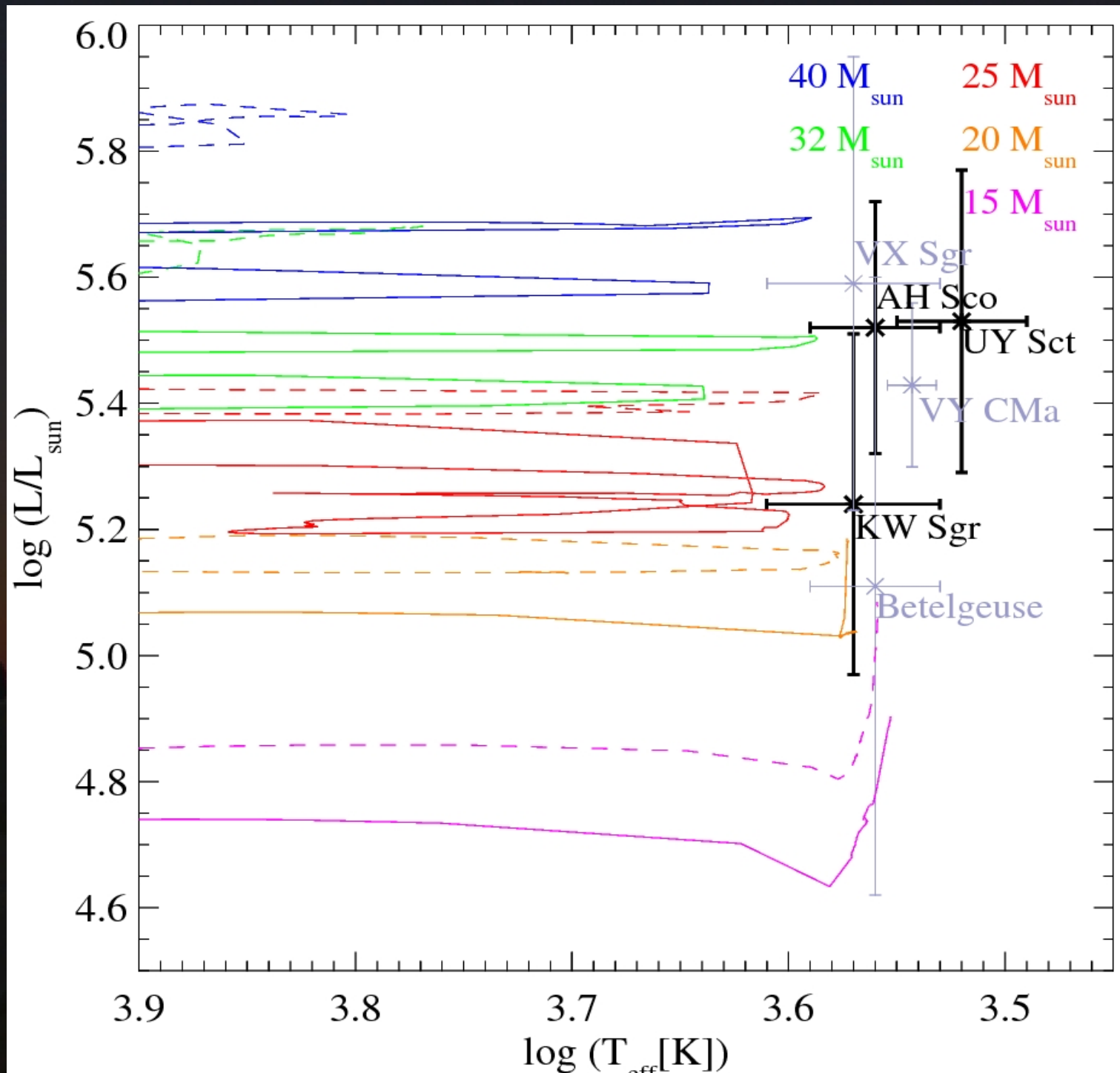
- Betelgeuse: $\theta = 42.29 \pm 0.06$ mas (Ohnaka et al. 2009, 2011)
 $d = 197 \pm 47$ pc (Harper et al. 2008)
 $f_{\text{bol}} = (1.07 \pm 0.11) 10^{-11}$ W m² (by us)
sp \rightarrow M2 lab
- VX Sgr: $\theta = 8,82 \pm 0.5$ mas (Chiavassa et al. 2010)
 $d = 1570 \pm 270$ pc (Chen & Shen 2008)
 $f_{\text{bol}} = (5.00 \pm 0.50) 10^{-9}$ W m² (by us)
sp \rightarrow M4 Ia (Humphreys et al. 1972)

Fundamental parameters

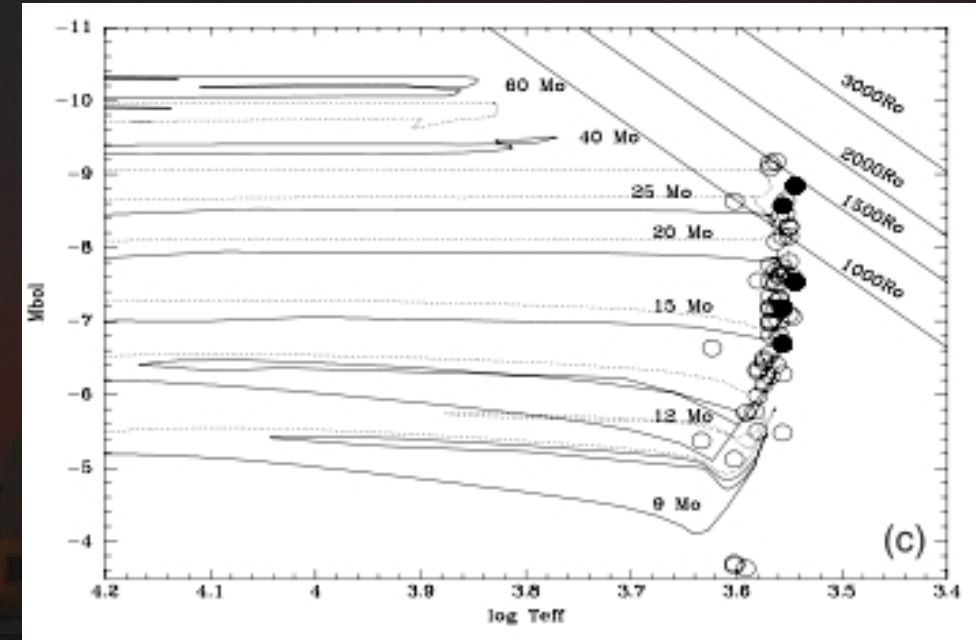


Our values confirm the calibrations by Levesque et al. and van Belle et al. KW Sgr and Betelgeuse are in very good agreement with the scale by Levesque et al., while the cooler sources show a larger scatter, but are consistent with these calibrations within $1-2\sigma$. This scatter may be caused by an erroneous spectral calibration or by a larger error of the bolometric flux.

Fundamental parameters



Location of RSGs in the HR diagram before (top) and after (bottom) the spectrophotometric correction by Levesque (Levesque et al. 2005)



Independent confirmation of Levesque et al. (2005) results using, spetro-interferometry data+PHOENIX model, instead of spetro-photometry+MARCS models

Position of AH Sco, UY Sct, KW Sgr (blue), Betelgeuse, VY CMa and VX Sgr (black) in the Hertzsprung-Russell (HR) diagram with recent evolutionary tracks obtained by Ekström et al. (2012)

Atmosphere structure

- The opacity of CO are well implemented in the PHOENIX models, but the extension of these molecular layers are too compact in the models compared to our observations.
- An important ingredient for understand the formation of stellar winds of cool giants and supergiants is the levitation of the gas to radii where dust particles can condense and be accelerated by radiative pressure.

In the case of AGB stars, it has been established that pulsation-induced shock waves lead to very extended atmospheres that reach to radii of a few photometric radii (Jeong et al 2003, Ireland et al. 2004, 2008, 2011).



The wavelength dependence of the visibility spectra observed in our work (RSGs) is similar to the observation of Mira variable AGB stars (Wittkowski et al. 2011). Although the pulsation amplitude of RSGs are lower than Mira stars, we speculate that for our targets is the same process.

Atmosphere structure

- Convection has been discussed as a possible process to dredge up material to higher layers and to produce surface inhomogeneities and shock waves in the photosphere (Chiavassa et al. 2011) .

↓
Problem...

* 3D convection simulation have been compared to VX Sgr and did not show the typical observed wavelength dependence of the visibility function at the positions of the water and CO bands.

* The time variation of the continuum data of Betelgeuse (Ohnaka et al. 2011) is much smaller than the maximum variation predicted by current 3D convection simulations.

* The current models it is not clear whether convective motion is strong enough to explain the motion detected at extended layers up to 1.4 stellar radii, where the convective flux is low (Chiavassa et al. 2011).

Conclusions

- ✗ Evidence of extended atmosphere with an envelope of water and CO layers.
- ✗ The models don't predict the visibility well: The model atmosphere is too compact when compared with the observations. This may be caused by pulsation and/or convection, which are not included in the models.
- ✗ The targets are located close to the red limits of the Hayashi limit of Ekström tracks. UY Sct and AH Sco are close to the theoretical track with initial mass of 25-30 M_{sun} with rotation. KW Sgr are close of 20-25 M_{sun} with rotation.

Future Work

- ✗ We want to extend this sample to more RSGs (better calibration of the effective temperature scale) and other regions of the HR diagram (red giants).
- ✗ Comparison to dynamic models and convection simulations.

A construction site at dusk. In the background, a large, multi-story building is under construction, with its skeletal frame visible against the darkening sky. The foreground shows a concrete slab with several red-painted markings, including a large octagon and several smaller circles. The overall scene is dimly lit, with the warm glow of the setting sun providing the primary light source.

Thanks